
**Indoor Airflow Patterns,
Dispersion of Human
Exhalation Flow and Risk of
Airborne Cross-Infection
between People in a Room**

Indoor Airflow Patterns, Dispersion of Human Exhalation Flow and Risk of Airborne Cross-Infection between People in a Room

PhD Thesis by

Inés Olmedo Cortés

*Department of Civil Engineering,
The Faculty of Engineering and Science,
Aalborg University, Aalborg, Denmark*


River Publishers
Aalborg

ISBN 978-87-92982-24-7 (e-book)

Published, sold and distributed by:

River Publishers

P.O. Box 1657

Algade 42

9000 Aalborg

Denmark

Tel.: +45369953197

www.riverpublishers.com

Copyright for this work belongs to the author, River Publishers have the sole right to distribute this work commercially.

All rights reserved © 2012 Inés Olmedo Cortés.

No part of this work may be reproduced, stored in a retrieval system, or transmitted in any form or by any means, electronic, mechanical, photocopying, microfilming, recording or otherwise, without prior written permission from the Publisher.

Preface

This thesis was written as a part of a PhD study during the past three years in a Joint-Degree Cooperation between the Department of Chemical Physics and Applied Thermodynamics, Córdoba University, Spain and the Department of Civil Engineering, Aalborg University, Denmark. The thesis is presented as a collection of the following seven peer-reviewed articles published in journals and conferences and the extended summary of those.

- Paper I** Olmedo, I., Nielsen, P.V., Ruiz de Adana, M., Grzelecki, P. and Jensen, R.L. (2010) Study of the human breathing flow profile in a room with three different ventilation strategies. Proceedings of the 16th ASHRAE IAQ Conference “*Airborne Infection Control - Ventilation, IAQ & Energy*”, Kuala Lumpur/Malaysia 10-12 November 2010.
- Paper II** Nielsen, P.V., Olmedo, I., Ruiz de Adana, M., Grzelecki, P. and Jensen, R.L. (2012) Airborne Cross-Infection Risk between Two People Standing in Surroundings with a Vertical Temperature Gradient. *HVAC&Research*, 18(4):1-10 (doi: 10.1080/10789669.2011.598441)
- Paper III** Olmedo, I., Nielsen, P.V., Ruiz de Adana, M. and Jensen, R.L. (2011) Airflow pattern generated by three air diffusers: Experimental and visual analysis. Proceedings of the 6th Mediterranean Congress of Climatization, Madrid/Spain 2-3 June 2011.
- Paper IV** Olmedo, I., Nielsen, P.V., Ruiz de Adana, M., Grzelecki, P. and Jensen, R.L. (2011) Experimental study about how the thermal plume affects the air quality a person breathes. Proceedings of the 12th International Conference on Air Distribution, Trondheim/Norway 19-22 June 2011.
- Paper V** Olmedo, I., Nielsen, P.V., Ruiz de Adana, M., Grzelecki, P. and Jensen, R.L. (2012) Distribution of exhaled contaminants and personal exposure in a room using three different air distribution strategies. *Indoor Air*, 22(1): 64-76 (doi: 10.1111/j.1600-0668.2011.00736.x.)
- Paper VI** Olmedo, I., Nielsen, P.V., Ruiz de Adana, M. and Jensen, R.L. (2012) The risk of airborne cross-infection in a room with vertical low-velocity ventilation. *Indoor Air* doi: 10.1111/j.1600-0668.2012.00794.x.
- Paper VII** Olmedo, I. and Nielsen, P.V. (2010) Analysis of the IEA 2D test. 2D, 3D, steady or unsteady airflow? Technical report. Series number 106, Department of Civil Engineering, Aalborg University.

The present thesis “Indoor airflow patterns, dispersion of human exhalation flow and risk of airborne cross-infection between people in a room” is the outcome of the research of a PhD study from October 2008 to January 2012. The study was supervised by Professor Manuel Ruiz de Adana at Córdoba University and by Professor Peter V. Nielsen at Aalborg University. First of all I would like to thank my two supervisors for fruitful input during my study, their positive attitude and for taking time to discuss my problems during all this time.

Professor Manuel Ruiz de Adana deserves my gratitude for his support and encouragement throughout the study. Many thanks to the people at Córdoba University for the good moments we have spent together. The help of Simon with the revision of the English is greatly appreciated.

Special thanks should be directed to Professor Peter V. Nielsen who hosted me at Aalborg University for nine months and always was positive, attended to my queries and taught me so many things during this thesis. Thanks for giving me the opportunity to work with you. All the department of Civil Engineering at Aalborg University deserves my gratitude for always welcoming and treating me as one of them at their department during my stays there. Thanks to Rasmus L. Jensen for his more than valuable help at the laboratory and technical explanations. I would also like to thank my colleague Piotr Grzelecki for the fruitful cooperation in the laboratory during my first stay in Aalborg. The friendly environment at Aalborg University cannot be forgotten, so thanks to all my friends there who made my stays joyful and very productive. Jytte Smedegaard also always made me feel at home in Aalborg, thanks for your time, your help, your support and the talking time since the first day I arrived there.

My family deserves special thanks for all their support, and patience and for always believing in me during these years. Finally, I would like to thank Sele for all his support, patience, understanding, constructive comments and for his love and companionship during these last years. All this work would have been impossible without them.

Finally, I must acknowledge that this thesis has taught me not only many technical things but it has also made me grow as a person and enrich my life mostly because of all the people who have been with me during these three years. Thanks to everybody!

Córdoba, February 2012

Inés Olmedo

Summary in English

In recent years, an interest in understanding the mechanisms of cross-infection between people in the same room has increased significantly. The SARS (*Severe Acute Respiratory Syndrome*) outbreak occurred in Asia in 2003 reopened the study of the airborne disease transmission as one of the most prevalent transmission routes.

Airborne cross-infection of diseases is caused by the transmission of pathogens, such as viruses or bacteria, between people and across environments. When a person is breathing, talking, sneezing or coughing, small particles, which may carry biological contaminants, are spread in the air. These tiny particles or droplet nuclei can follow the air flow pattern in the room and produce high contaminant concentration in different areas of the indoor environment. This fact can provoke a high exposure to exhaled contaminants and a risk of cross-infection to a susceptible person situated in the same room.

Abundant evidence shows that the air flow distribution systems play a crucial role in the dispersion of these human exhaled contaminants. However, there are many parameters that influence the cross-infection risk between people situated close to each other in a ventilated room, such as: relative position and separation distance between people, difference in height between them, level of activity, breathing function or process (breathing frequency, exhalation through the mouth or through the nose, coughing, sneezing) or air velocity and turbulence level in the micro-environment around the persons.

This thesis analyzes some of these parameters in the influence of cross-infection risk between two people in a room, which are simulated by two breathing thermal manikins. One of the manikins is considered the source of contaminants, which is exhaling contaminated air through the mouth. The influence of different ventilation strategies in the personal micro-environment, the direction of the human exhalation flow and the dispersion of exhaled contaminants has also been studied.

Several experimental tests in a full-scale test room have been carried out in order to study the cross-infection risk between two people in a room. Different ventilation strategies and different separation distances, and relative positions, between the manikins produce different levels of contaminant exposure to the susceptible person (target manikin). These results have been discussed and carefully analyzed within this thesis.

Dansk Resumé

Der har i de seneste år været en stigende interesse for at undersøge og forstå mekanismerne i krydsinfektion imellem folk, som opholder sig i det samme lokale. SARS-hændelsen (Severe Acute Respiratory Syndrome) som fandt sted i Asien i 2003 betød, at studier af luftbårne transmissionsruter for sygdomme blev et meget aktivt forskningsområde.

Luftbåren krydsinfektion af sygdomme foregår ved transmission af patogener som virus eller bakterier imellem personer i indemiljøet. Når en person ånder, taler, nyser eller hoster, vil små biologisk forurenede partikler spredes i luften. Disse små partikler (droplet nuclei) følger luftstrømningsmønstret i lokalet, og de kan danne høje koncentrationer i forskellige områder af indemiljøet. Dette kan betyde, at der kan opstå en høj eksponering for udåndet forurening og derfor en risiko for krydsinfektion af en påvirkelig person, som befinder sig i samme rum.

Mange hændelser viser, at luftfordelingssystemerne spiller en væsentlig rolle i fordelingen af disse udåndede humane forureninger. Der er imidlertid mange parametre, som har indflydelse på risikoen for krydsinfektion imellem folk, som befinder sig tæt ved hinanden i et ventileret lokale, som for eksempel relativ position og afstand, forskel i højde, aktivitetsniveau, åndingsproces (åndingsfrekvens, udånding gennem mund eller gennem næse, hosten eller nysen) samt lufthastighed og turbulensniveau i mikromiljøet rundt om personer.

Afhandlingen analyserer nogle af disse parametres indflydelse på risikoen for krydsinfektion imellem to personer i et lokale, idet man betragter en af personerne som en kilde til smitte. Den syge person udånder forurenede luft igennem munden. De forskellige luftfordelingsstrategiers indflydelse på det personlige mikromiljø, retningen af en persons udånding og fordelingen af den udåndede forurening er undersøgt.

Der er udført adskillige forsøg for at undersøge risikoen for krydsinfektion i et fuldskala forsøgslokale, hvor to personer er simuleret ved hjælp af to termiske manikiner med åndingsfunktion. Forskellige ventilationsstrategier og forskellige afstande imellem manikinerne samt forskellige relative positioner giver en person (Target manikin) forskellig forureningspåvirkning. Resultaterne er diskuteret og analyseret i denne afhandling.

Resumen en español

En los últimos años ha surgido un especial interés en entender los mecanismos de transmisión de infecciones cruzadas entre personas. El *Síndrome Respiratorio Agudo Severo* (SARS, por sus siglas en inglés) que tuvo lugar en Asia en el año 2003 reabrió el estudio de la transmisión de diferentes enfermedades vía aérea como una de las rutas de transmisión más activas.

Las infecciones cruzadas entre personas son causadas por la transmisión de patógenos, como virus o bacterias, entre personas en ambientes interiores. Cuando una persona respira, habla, estornuda o tose, pequeñas partículas, denominadas “droplet nuclei”, que pueden contener contaminantes biológicos, son dispersadas en el aire. Estas pequeñas partículas pueden seguir las corrientes de flujos de aire dentro de una habitación y provocar altas concentraciones de contaminantes en diferentes áreas dentro de un recinto interior. Este hecho puede provocar una alta exposición a contaminantes exhalados y un riesgo de infección cruzada a personas susceptibles de ser contagiadas situadas en la misma habitación.

Existen numerosas evidencias de que los sistemas de ventilación y distribución de aire juegan un papel crucial en la dispersión de los contaminantes exhalados por personas en recintos interiores. Sin embargo, existen muchos parámetros que influyen en el riesgo de infección cruzada entre personas en una habitación climatizada, como son: la posición relativa entre las personas, la distancia de separación entre ellas, su diferencia de alturas, su nivel de actividad, las funciones respiratorias de las personas (si exhalan el aire por la nariz o por la boca, si se produce un estornudo, etc.) o la velocidad y nivel de turbulencia del aire en el micro-ambiente alrededor de las personas.

El objetivo principal de esta tesis es analizar la relación de alguno de los parámetros detallados anteriormente con el riesgo de infección cruzada que se puede generar entre personas dentro de una habitación. La influencia de diferentes estrategias de climatización sobre el micro-ambiente de las personas, sobre la dirección de la exhalación y sobre la dispersión de contaminantes exhalados en el aire ha sido también estudiada.

Se han realizado numerosos estudios experimentales considerando dos personas dentro de una misma habitación climatizada mediante diferentes sistemas. La simulación de las personas se ha llevado a cabo mediante maniqués térmicos que incluían funciones respiratorias. La exhalación de uno de ellos era considerada la fuente biológica de contaminantes mientras que el otro era la persona susceptible de ser contagiada a través del aire. Los estudios experimentales incluyen diferentes posiciones relativas entre personas y distintas distancias de separación.

Los resultados muestran una significativa influencia de la distancia de separación y la posición relativa entre las personas en la transmisión de patógenos por el aire y el riesgo de infección cruzada entre personas. Algunos de los sistemas de ventilación de aire considerados hasta ahora como adecuados en la prevención de este tipo de contagios a través del aire, como es el sistema de ventilación vertical a baja velocidad, no han mostrado especial protección contra las infecciones cruzadas en los ensayos experimentales. La exposición frente a contaminantes exhalados varía significativamente entre los distintos casos y los resultados han sido analizados minuciosamente a lo largo de esta tesis. Los resultados obtenidos dejan patente la influencia de las condiciones interiores de aire generada por los distintos sistemas de climatización en la transmisión de patógenos a través del aire en recintos interiores, en la calidad de aire que proporcionan a las personas y por lo tanto en el riesgo de infecciones cruzadas que se puede generar.

Nomenclature

a_0	area of the manikin's mouth, m ²
A_0	opening area of a jet, m ²
Ar	Archimedes number
c	tracer gas concentration, ppm
c_0	peak concentration at the manikin's mouth, ppm
c_R	tracer gas concentration in the return, ppm
c_s	tracer gas concentration surrounding the manikin, ppm
c_x	tracer gas concentration at a horizontal distance from the mouth, ppm
c_{chest}	tracer gas concentration at the chest, ppm
c_{exp}	tracer gas concentration in the inhalation, ppm
c_{10}	tracer gas concentration 0.10 m above the head, ppm
g	gravitational acceleration (m ² /s)
H	height of the test room, m
K_c	characteristic concentration constant
K_{exp}	characteristic velocity constant
K_v	centre velocity decay constant for a jet
n_1	characteristic velocity exponent
n_2	characteristic concentration exponent
T	absolute air temperature, K
T_0	exhaled air temperature, K
T_{amb}	air temperature at the height of the manikin's mouth, K
T_{in}	supply air temperature, K
T_{out}	return air temperature, K
u_0	initial velocity of a jet and peak velocity in the manikin's mouth, m/s
u_x	peak velocity at a horizontal distance from the manikin's mouth, m/s
x	horizontal distance, m
z	vertical distance, m
β	volume expansion coefficient
ΔT	temperature difference between the exhalation flow, T_0 , and the ambience in the room, T_{amb}

Contents

Preface	iii
Summary in English.....	v
Dansk Resumé.....	vi
Resumen en español.....	vii
Nomenclature.....	viii
Contents	ix
List of figures	xiii
List of tables	xvii
CHAPTER 1 - Introduction	1
1.1 Ventilation strategies in indoor environments.....	1
1.1.1 Displacement ventilation.....	2
1.1.2 Mixing ventilation.....	2
1.1.3 Unidirectional low-velocity flow ventilation.....	3
1.2 Influence of people in the airflow patterns.....	4
1.2.1 People as a heat load.....	4
1.2.2 People as a source of biological contaminants.....	5
1.3 Transmission routes of diseases.....	6
1.3.1 Direct contact with people.....	6
1.3.2 Large droplet contact.....	7
1.3.3 Airborne transmission.....	8
1.4 The importance of ventilation systems in preventing airborne cross-infections.....	9
1.5 Layout of the thesis.....	9
CHAPTER 2 - Materials and method	11
2.1. Experimental materials and facilities.....	11
2.1.1 Test room and measurements facilities.....	11
2.1.2 Description of the diffusers.....	12

2.1.3	Manikin model of a person	13
2.1.4	Simulation of the human breathing	14
2.2.	Experimental method	16
2.2.1	Experimental set-up	16
2.2.1	Data process	16
CHAPTER 3 - Airflow patterns generated in the room		17
3.1	Importance of the air supply conditions.....	17
3.2	Materials and methods.....	18
3.3	Airflow pattern for the mixing diffuser	18
3.3.1	Turbulent isothermal free jets	19
3.3.2	Airflow and velocity decay	20
3.4	Airflow pattern for the displacement diffuser.....	22
3.5	Airflow pattern for the low-velocity vertical diffuser.....	23
3.6	Discussion of the results	24
CHAPTER 4 - Dispersion of human exhaled contaminants in a room		25
4.1	Experimental conditions in the room with one manikin.....	25
4.2	Influence of the thermal plume on the air quality a person breathes.....	28
4.3	Study of the exhalation flow	30
4.3.1	Thermal conditions in the room	30
4.3.2	Centreline of the exhalation flow.....	31
4.3.3	Airflow model of exhalation flows	32
4.3.4	Velocity and concentration decay	34
4.4	Conclusions	38
CHAPTER 5 - Cross-infection between people in a room.....		41
5.1	Evidences of cross-infection risk in indoor environments.....	41
5.2	Methods	42
5.3	Two manikins within a room with displacement ventilation.....	43
5.3.1	Layout of the tests	43
5.3.2	Results.....	45
5.3.3	Comparison of the personal exposure levels.....	47
5.4	Two manikins within a room with mixing ventilation	48
5.4.1	Layout of the tests.....	48
5.4.2	Results	49
5.5	Two manikins within a room without mechanical ventilation	49

5.6 Two manikins within a room with low velocity vertical ventilation	50
5.6.1 Layout of the tests.....	50
5.6.2 Results	52
5.7 Comparison of the results for the different ventilation strategies.....	54
CHAPTER 6 - Conclusions and future work.....	57
Bibliography	59
Appendix A - Calibration of the equipment.....	67
A. 1 Calibration of the thermocouples.....	67
A.2 Calibration of the anemometers.....	68
Appendix B - Study of the human breathing flow profile in a room with three different ventilation strategies.....	71
Appendix C - Airborne cross-infection risk between two people standing in surroundings with a vertical temperature gradient	73
Appendix D - Airflow pattern generated by three air diffusers: Experimental and visual analysis	75
Appendix E - Experimental study about how the thermal plume affects the air quality a person breathes.....	77
Appendix F - Distribution of exhaled contaminants and personal exposure in a room using three different air distribution strategies	79
Appendix G – The risk of airborne cross infection in a room with vertical low-velocity ventilation	81
Appendix H - Analysis of the IEA 2D test. 2D, 3D steady or unsteady airflow?	83

List of figures

Figure 1.1	Picture of the displacement ventilation airflow pattern generated in a room occupied with one person and the most common characteristics of this ventilation system.....	2
Figure 1.2	a) Airflow pattern close to a wall opening, b) Picture of the mixing ventilation airflow pattern generated in a room occupied by a person	3
Figure 1.3	Picture of a downward airflow pattern generated in a room occupied with one person a) Front view, b) Lateral view	3
Figure 1.4	Model of the heat and the thermal plume generated by the metabolism of a person. T_s is the superficial temperature of the person and T_{amb} the ambient temperature	4
Figure 1.5	Relation between the number of particles expelled and the exhalation flow rate during a normal exhalation (Schwartz et al., 2010)	5
Figure 1.6	a) Flash picture of a human sneeze, b) Cough flow rate variation in time (Gupta et al., 2009).....	6
Figure 1.7	The Wells evaporation falling curve of droplets (Wells 1934)	7
Figure 1.8	a) Dispersion of exhaled particles in a room with two people, in red the person exhaling the contaminants and in blue the susceptible person of being infected, b) Relation between the particles size and the region of the human respiratory system that the particles can reach (Yang et al., 2011).....	8
Figure 2.1	Sketch of the test room. Semi-circular displacement diffuser (DD), square mixing diffuser (MD), textile diffusers (TD), return openings for the mixing ventilation and displacement ventilation cases (E), return opening for the vertical ventilation with the textile diffusers (E2).....	12
Figure 2.2	Description and size of the four-way ceiling mounted mixing diffuser	13
Figure 2.3	Semicircular wall-mounted displacement diffuser a) Picture, b) Size	13
Figure 2.4	a) Picture of the source manikin, b) Detailed description of the manikins' size (Bjørn (1999)).....	14
Figure 2.5	Picture of the artificial lungs a) for the source manikin, b) for the target manikin.....	15
Figure 3.1	a) Sketch of the test room and location of the diffusers and exhaust (D, displacement diffuser; M, mixing diffuser; T, textile diffuser; E, exhaust openings for the mixing and displacement ventilation tests; E2, exhaust opening used with the textile diffuser), b) Placement of the diffusers and	

radiator in the room (R1, position of the radiator for the tests with the mixing and displacement diffuser; R2, position of the radiator for the test with the textile diffuser)	18
Figure 3.2 Picture of an isothermal jet	19
Figure 3.3 Dimensionless velocity versus dimensionless distance for a free jet (Reproduced from Nielsen, 1995)	20
Figure 3.4 a) Velocity profile generated by the ceiling-mounted mixing diffuser, b) Airflow smoke visualization.....	20
Figure 3.5 Placement of the anemometers respect to the diffuser (grey) and velocity results obtained for each anemometer (red).....	21
Figure 3.6 Log-log graph representing the velocity decay of the mixing diffuser	21
Figure 3.7 a) Velocity profile generated by the wall-mounted displacement diffuser along at horizontal line at 0.01 m from the floor, b) Airflow smoke visualization.....	22
Figure 3.8 a) Placement of the measuring line T1, b) Velocity profile measured at 0.8 m the diffuser along the line T1.....	23
Figure 3.9 Smoke visualization of the flow at three instants of time a) 1s, b) 2.5 s, c) 4.5 s	24
Figure 4.1 Exhalation velocity profiles for the two groups of cases. a) <i>Group A</i> , b) <i>Group B</i>	26
Figure 4.2 Placement of the source manikin (S), radiator (R), vertical lines, L1 and L2 and diffusers a) Mixing ventilation (M) and without mechanical ventilation, b) Displacement ventilation (D), c) Vertical ventilation with the textile diffuser (T) for the downward flow position, d) Vertical ventilation with the textile diffuser (T) for the upward flow position	27
Figure 4.3 Concentration values along the vertical lines. a) L1 in the room, b) L2 at 0.50 m from the manikin	29
Figure 4.4 Concentration values in the thermal plume of the manikin at the height of the hips, chest and in the inhalation.....	29
Figure 4.5 Vertical temperature distributions in the room along L1 for the four cases with mechanical ventilation.....	30
Figure 4.6 Smoke visualization of the exhalation jet in the displacement ventilation case and placement of the probes along the centreline at different time intervals a) 0.1 s, b) 0.2 s, c) 0.35 s, d) 0.5 s and e) 0.65 s	31
Figure 4.7 Placement of the anemometers and concentration tubes along the centreline of the exhalation flow respect to the manikin for each case studied	32
Figure 4.8 Centreline of the exhalation jets for the five ventilation principles	33
Figure 4.9 Velocity and concentration decay of the exhalation jet for the five cases studied. a) Non-mechanical ventilation, b) Mixing ventilation, c) Displacement ventilation, d) Vertical ventilation in the downward flow area, e) Vertical ventilation in the upward flow area.....	35
Figure 4.10 Velocity and concentration level along the centreline of the exhalation jet versus distance to the mouth in a log-log graph for the different ventilation strategies. a) non-mechanical ventilation, b) mixing ventilation, c) displacement ventilation, d) vertical ventilation with downward flow, e) vertical ventilation with upward flow.....	38
Figure 4.11 Comparison of the velocity and concentration decays in a log-log graph.....	38

Figure 5.1	Sketch of the test room with the source (S) and the target (T) manikins and location of the concentration tubes at the chest (c_{chest}), the inhalation (c_{exp}) and above the manikin (c_{I0}). The separation distance between the manikins in the pictures is 0.80 m. All measurements in meters.....	42
Figure 5.2	Relative positions of the manikins (source in red and target in blue) a) Manikins standing face to face, b) Manikins standing face to side, c) Manikins standing face to back, d) Source manikin seated and target manikin standing	43
Figure 5.3	Experimental setup with the two manikins (T, target manikin; S, source manikin) for the tests with the displacement diffuser (D) and the mixing diffuser (M), vertical measuring line (L1) and radiator (R). The position of the target manikin was moved to obtain the different separation distances. All measurements in meters	44
Figure 5.4	Vertical temperature distributions at L1 for the displacement and mixing ventilation tests.....	45
Figure 5.5	Comparison of the exposure concentration values in the inhalation (c_{exp}/c_R), the chest (c_{chest}/c_R), and above the target manikin (c_{I0}/c_R) for the displacement ventilation tests a) test 1, b) test 2, c) test 3, d) test 4	46
Figure 5.6	Comparison of the personal exposure obtained for the four displacement ventilation cases: face to face, face to side, face to back and with the source manikin seated.....	47
Figure 5.7	Concentration measurement over 280 minutes for two displacement ventilation tests a) test 1 (face to face), b) test 2 (face to back).....	48
Figure 5.8	Comparison of the exposure concentration values in the inhalation (c_{exp}/c_R), the chest (c_{chest}/c_R), and above the target manikin (c_{I0}/c_R) for the mixing ventilation tests a) test 1, b) test 2	49
Figure 5.9	Comparison of the exposure concentration values in the inhalation (c_{exp}/c_{chest}) and above the target manikin (c_{I0}/c_{chest})	50
Figure 5.10	Layout of the room with the radiator (R), target manikin (T), source manikin (S) and textile diffuser (TD), a) test 1, b) test 2, c) test 3	52
Figure 5.11	Comparison of the exposure concentration values in the inhalation (c_{exp}/c_R), the chest (c_{chest}/c_R), and above the target manikin (c_{I0}/c_R) for the low-velocity vertical ventilation tests a) test 1, b) test 2, c) test 3	53
Figure 5.12	Comparison of the personal exposure concentration values for the different ventilation systems studied: displacement ventilation (DV), mixing ventilation (MV) and low-velocity vertical ventilation (grey area).....	54

List of tables

Table 2.1 Breathing functions of the two manikins for the different ventilation strategies: non-mechanical ventilation (NV), mixing ventilation (MV), displacement ventilation (DV) and low-impulse vertical ventilation placing the manikins in the downward flow area (DWF) and in the upward flow area (UWF).....	15
Table 3.1 Position of the anemometers along the horizontal line, T1.....	23
Table 4.1 Breathing functions of the source manikin	26
Table 4.2 Heat load released by the manikin for the study of the thermal plume.....	27
Table 4.3 Position of the manikin with the different ventilation strategies	28
Table 4.4 Position of the anemometers and concentration tubes along the centreline of the exhalation flow	32
Table 4.5 Temperature data obtained for the five ventilation strategies, $T_0=34$ °C.....	34
Table 4.6 Characteristic velocity and concentration constants and exponents for the exhalation jets.....	36
Table 5.1 Experimental tests with two manikins and displacement ventilation	44
Table 5.2 Experimental tests with two manikins and displacement ventilation	48
Table 5.3 Experimental tests with two manikins and low-impulse velocity ventilation.....	51

CHAPTER 1

Introduction

In this chapter the problem of cross-infection risk between people in indoor environments is presented. The route map of the thesis is outlined and the relationship of the represented publications to the subject matter of the study is pointed out. The main focus of the thesis has been on improving the understanding of how different ventilation systems can prevent us from a high exposure to exhaled contaminants and therefore a possible cross-infection risk in indoor environments. The results are based on experimental tests carried out in a full-scale test room. A description of different ventilation strategies, the human generation of exhaled contaminants, the routes of disease transmission and several parameters that influence the airflow patterns and the indoor environment conditions are presented.

1.1 Ventilation strategies in indoor environments

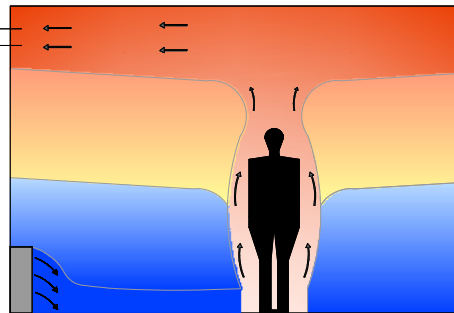
Since human beings are spending most of their time inside buildings, different ventilation strategies have been developed. The simplest one is the use of natural ventilation, which consists of renovating the indoor air of a building making fresh air pass through opened windows or doors. It does not require any device to move the air and therefore no energy is consumed. However, the characteristics and quality of the air are difficult to control since they depend on the outdoor and indoor ambient conditions. To avoid this problem and control the indoor conditions and air quality during the whole year and under different environmental conditions the HVAC (*Heating, Ventilation and Air Conditioning*) systems were developed.

The HVAC systems are supposed to create the right conditions of air temperature, velocity, humidity and quality in order to provide a comfortable and healthy indoor environment for people. The ventilation systems are also used to remove airborne particles or contamination generated inside a room, as for example aerosols or VOCs (*Volatile Organic Compounds*). To proportionate the desirable indoor conditions the air is cooled, heated and renovated in a central unit. After that, this air is directed through ducts and supplied to the indoor spaces or rooms through supply openings which can significantly vary the indoor air conditions and thermal environment in the area occupied by people. The way in which the air is supplied to the room, especially its velocity and momentum flow, together with the layout of the return openings, creates different airflow patterns, temperature distributions and indoor environments, and allows us to classify different air distribution systems. Short descriptions of the most used ones are presented in the

following sections.

1.1.1 Displacement ventilation

Displacement ventilation is a high efficiency air distribution system where the ventilation is driven by buoyancy force. The diffuser delivers cool air near the floor at a low velocity and temperature. The cool air initially drops as it leaves the diffuser and spreads across the room. At the same time, warm air in the room rises. Wherever there is a heat source in the room, e.g. a person, it creates a thermal plume, inducing cold air from the floor to the warm upper part of the room. The natural convective upward flow generated makes it appropriate to place the return openings in the upper part in order to allow the warmed air to leave the room. In the space between the cool air close to the floor and the warm air in the upper part of the room the air is thermally stratified. Figure 1.1 illustrates, with a short summary of its more common characteristics, the air distribution generated by this ventilation strategy in a room where a person is placed.



- ✓ Energy efficient
- ✓ Vertical temperature stratification
- ✓ Thermal comfort if the gradient is less than 3K/m
- ✓ Lack of draft, low air velocity

Figure 1.1 Picture of the displacement ventilation airflow pattern generated in a room occupied with one person and the most common characteristics of this ventilation system

This kind of system is very efficient in removing particles from the low part of the room, since the upward flow generated drives the contaminants to the upper part. In this way, this system generates a low clean air zone and a contaminated upper part in the room. However, a lock-up phenomenon of contaminants exhaled by a person has been reported by several authors (Brohus and Nielsen, 1996; Bjørn and Nielsen, 2002; Nielsen et al., 2009; Qian et al., 2006). The air exhaled by a person can remain stuck in a stratified layer in the surrounding of the person and produce high concentration of exhaled contaminants (Olmedo et al., 2011).

1.1.2 Mixing ventilation

The air movement in mixing ventilation is driven by the momentum flow generated by the supply opening. These supply devices are installed on the ceiling or in a wall at a certain height and generate a turbulent jet in front of them. This jet will entrain the air in the room generating a mixing process with the air into the room, see figure 1.2. The penetration distance of the jet will condition the maximum velocity in the occupied zone. The mixing

process creates a uniform temperature and contaminants distribution in the room (Jiang et al., 1992). In the occupied zone, the penetration distance of the jet will condition the maximum velocity and the contaminant concentration may be low due to the dilution process generated by this ventilation strategy (Jensen et al., 2001).

Figure 1.2(b) shows the general airflow pattern generated by a ceiling mounted ceiling diffuser in a room occupied by one person.

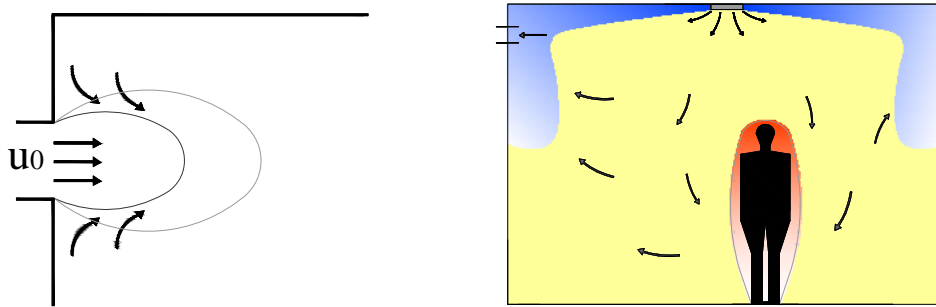


Figure 1.2 a) Airflow pattern close to a wall opening, where u_0 is the initial velocity of the jet, b) Picture of the mixing ventilation airflow pattern generated in a room occupied by a person

1.1.3 Unidirectional low-velocity flow ventilation

This ventilation system supplies air at a low velocity from a rather large inlet surface in a vertical or horizontal direction. When the air is supplied from the ceiling in a vertical direction, a downward “laminar” flow is created into the room, see figure 1.3.

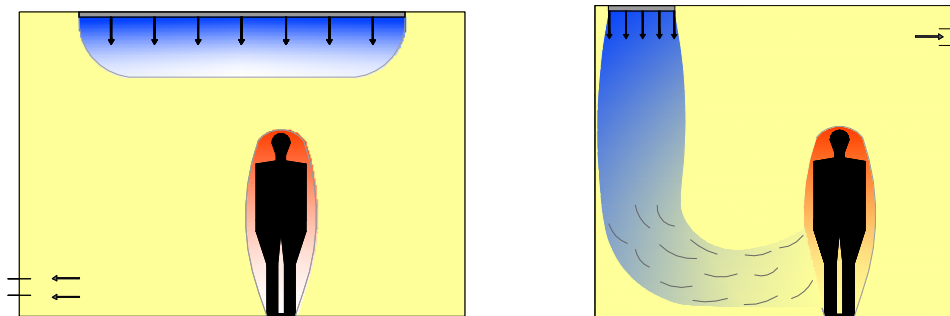


Figure 1.3 Picture of a downward airflow pattern generated in a room occupied with one person a) Front view, b) Lateral view

This system was developed for industrial clean rooms. It is considered one of the most efficient systems to control the dispersion of contaminants due to the large volume flow of clean air that can be applied without generating draught (Chow and Yang, 2004; Nielsen 2007). For that reason, it is supposed to be very effective removing pollutants from a room and it is recommended in some design guidelines for prevention of airborne disease (CDC 2004; CDC 2005). The unidirectional downward flow (piston flow) that they can create

drives the pollutants to the low part of the room where they are removed. However, the convective air movement generated by heat loads can create a mixing flow pattern in the room (Nielsen et al., 2007). If people are placed below the diffuser they can disturb the expected unidirectional “laminar” flow and generate a mixing process with the air. Placement of heat loads such as people, exhaust openings and obstacles in the room significantly influence the airflow pattern generated in the room (Qian et al., 2008).

1.2 Influence of people in the airflow patterns

The airflow pattern generated inside a room is not only created by the ventilation strategy but it is also influenced by the room geometry, obstacles and thermal loads, such as people, which occupy a room.

As people are the main occupants of buildings the indoor environment has to fulfil several conditions of thermal comfort and air quality to provide a comfortable and healthy environment to people (ISO 7730: 2005). However, occupants in a room are considered one of the most important heat loads and biological sources of contaminants. The following sections give a short description of the human metabolism and breathing functions that directly influence the indoor air conditions.

1.2.1 People as a heat load

The first aspect to consider about a person is that it is one of the most important thermal loads inside a building. Even when inactive, an adult will lose heat at a rate of about 90 watts as a result of his basal metabolism. Figure 1.4 shows a simplified model of the process by which the human body gives off heat.

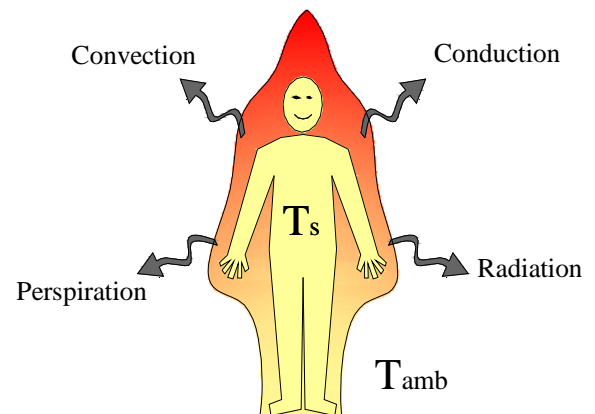


Figure 1.4 Model of the heat and the thermal plume generated by the metabolism of a person. T_s is the superficial temperature of the person and T_{amb} the ambient temperature

The heat transmission from a person to the environment is due to:

- ✓ Convective forces which are due to the temperature difference between the surface of a person and the ambience and varies depending on the clothes degree, and the ambient.
- ✓ Radiation, which is generated by all warm surfaces as an emission of radiate waves.
- ✓ Conduction, the heat released by a person is carried out through the stationary air that is adjacent to the surface of a person.
- ✓ Perspiration. This is a cooling mechanism that evaporates liquid surface (sweat) when the human body is surrounded by a higher temperature.

When a person is placed in a room which is being conditioned, the temperature of the human body generates a convective upward flow due to the temperature difference with the ambient temperature, which is known as thermal plume (Clark and Edholm, 1985; Craven and Settles, 2006). This thermal plume can condition the airflow pattern and the temperature distribution expected in the same room without any occupant.

1.2.2 People as a source of biological contaminants

Human beings can be considered one of the main sources of diseases since they are transmitted most of the times by a human to human contact. The normal human pulmonary functions such as breathing, coughing, talking or sneezing produce atomized fluids containing pathogens, i.e. viruses, bacteria or fungi. The spreading of infectious respiratory diseases in indoor environments is a consequence of a direct or indirect contact with these droplets.

The normal breathing function consists of an inhalation period, during which the air comes into the respiratory system until it reaches the lungs. Once there, the oxygen of the air passes to the human blood through millions of small membranes called alveoli. After that, the second part of the respiration, which is called exhalation, takes part. The air empty of oxygen leaves the human respiratory system to leave the way to another inhalation. This process is repeated by a person between 10-20 times per minute depending on the size, age and gender, among other factors of the person, and the variation of its air flow rate over the time is a sinusoidal function (Gupta et al., 2010).

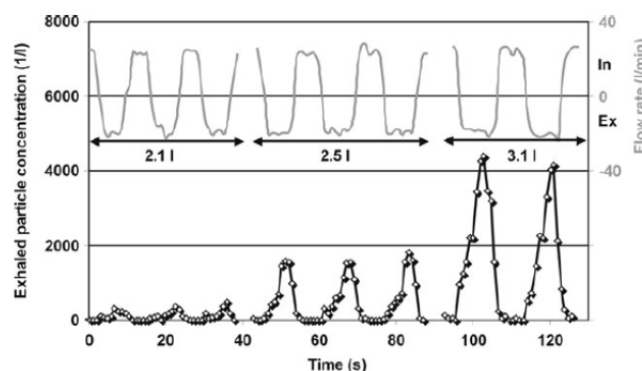


Figure 1.5 Relation between the number of particles expelled and the exhalation flow rate during a normal exhalation (Schwartz et al., 2010)

During the exhalation process human aerosol containing possible biological contaminants are spread in the air. Depending on the breathing function, the number of particles generated changes. A larger flow rate generates a larger number of exhaled particles, see figure 1.5.

Human sneeze and cough can be considered one of the most important sources for spreading respiratory infectious diseases. Much research has been done considering the human cough as a source of communicable diseases (Badeau et al., 2002; Zhu et al., 2006a). The droplet generation of a cough is significantly high and its initial high speed makes the exhaled particles flow long distances unaffected by the indoor airflow (Zhu et al., 2006b; Zhu and Kato, 2006; Chao et al., 2009; Zhao et al., 2005).

Figure 1.6 shows the particles expelled by a human cough and the flow rate variation in time. Gupta et al., 2009 characterized the human cough flow rate and direction with 25 human subjects. They also provided very useful information about the human mouth opening size during a normal cough.

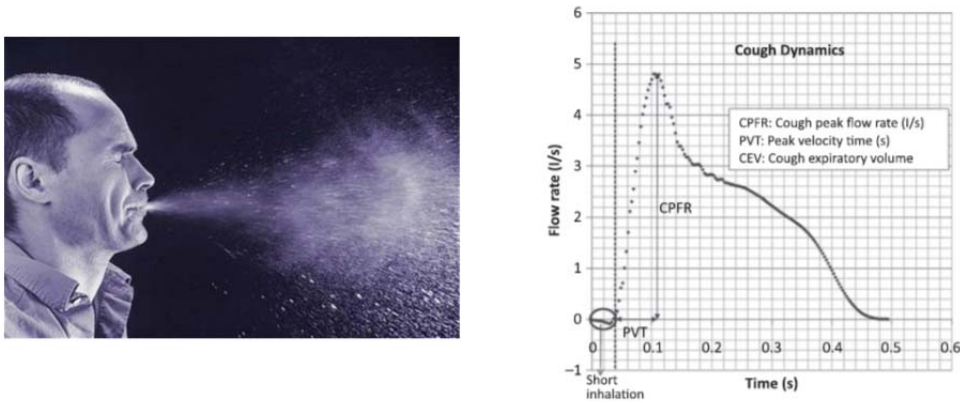


Figure 1.6 a) Flash picture of a human sneeze, b) Cough flow rate variation in time (Gupta et al., 2009)

The content and especially the size of the human exhaled particles determine the route of transmission of disease. The following section describes the transmission routes of diseases that are related with human exhaled particles.

1.3 Transmission routes of diseases

The daily contact with other humans makes us susceptible to pathogens, bacteria and viruses that affect our health. The routes of transmission of diseases are different and are described briefly in the following sections.

1.3.1 Direct contact with people

This route of disease transmission is not directly connected with exhaled particles by a person. It occurs when there is physical contact between a susceptible person and an infected person or contaminated object or surface.

Many illnesses spread through contact transmission, e.g.: chicken pox, common cold, conjunctivitis, Hepatitis A and B, herpes simplex, influenza, measles or mononucleosis. The way of preventing this way of transmission is by the use of physical barriers, such as gloves and the cleaning of contaminated, frequently touched surfaces, as well as washing hands.

A possible direct transmission route is also possible through vectors such as mosquitos, which can transport human fluids (blood) from one person to another.

1.3.2 Large droplet contact

Expiratory droplets expelled during coughing, sneezing, laughing or talking are pathogen carriers that can provoke a cross-infection risk between people in two ways. Firstly, by a direct contact of a person with a contaminated large droplet exhaled and spread in the air by an infected person. This route of transmission is quite common in hospitals wards or clinical sites, where the exposure to aerosol exhaled by infectious people is high (Chen et al., 2010). The common way to prevent this route of transmission is the use of masks and other physical barriers (Tang et al., 2009). The second way in which large expelled droplets can provoke a risk of infection to a healthy person is by indirect contact, provoking the contamination of a surface or object. Larger droplets fall down due to gravitational effect and can be deposited in different surfaces (Qian and Li, 2010; Wan and Chao 2007; Xie et al., 2007; Chao et al., 2008). Once there, the bacterial cells or viruses contained in the droplets can remain for long periods. The possible cross-infection is caused when a person comes in contact with the contaminated large droplets deposited. The critical size of which is considered a large droplet is a function of many different parameters such as the ambient humidity. According to the Wells evaporation curve, see figure 1.7, which relates the droplet size with the time to fall down, larger droplets are considered to be droplets larger than $100\mu\text{m}$, which fall down quickly due to gravitational effect. However, a recent study by Xie et al., 2007 determines the size of the large droplets between 60 and $100\mu\text{m}$ and Chao et al., 2008 also determined that large droplets larger than $87.5\mu\text{m}$ settle down due to the gravitational effect.

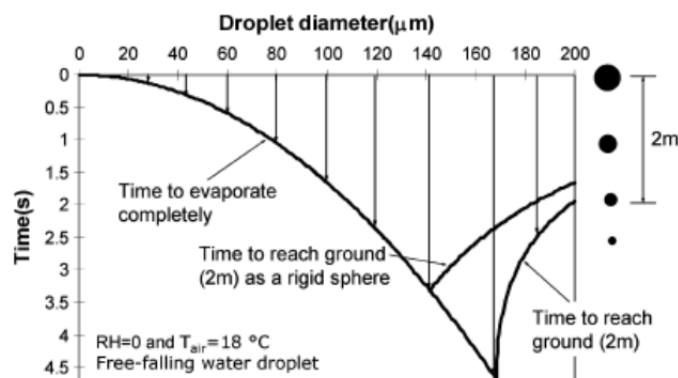


Figure 1.7 The Wells evaporation falling curve of droplets (Wells 1934)

1.3.3 Airborne transmission

Airborne transmission of infections is considered one of the major infectious routes of different diseases such as influenza, tuberculosis or measles. While contaminated exhaled large droplets fall due to gravitational effect, small droplets or droplet nuclei carrying biological contaminants remain in the air and follow the air stream dispersing in the air (Chao et al., 2008; Wan et al., 2009; Chen and Zhao 2010), see figure 1.8(a). Consequently, the exhaled air may be effective in the transportation of organisms, such as viruses that may be carried in these very fine droplets see Nicas et al. (2005) and Morawska (2006). When these particles reach the inhalation region of a person, they are inhaled and conducted to the lungs. However, the human respiratory system has several protective mechanisms such as the mucous in the nasal cavity or tiny hairs called cilia in the trachea. These systems avoid the particles to reach the lungs and prevent a blood infectious. The success of these human protective systems partly depends on the size of the particles. Yang et al., 2011 studied the relation between the size of the particles and the reach of these particles inside the human respiratory system, see figure 1.8(b). Most of the larger particles, close to 100 μm , are filtered in the nasal cavity, while very fine and small particles can easily reach the lungs. This fact makes the tiny exhaled contaminant particles one of the most active, invisible and dangerous airborne route of transmission of diseases.

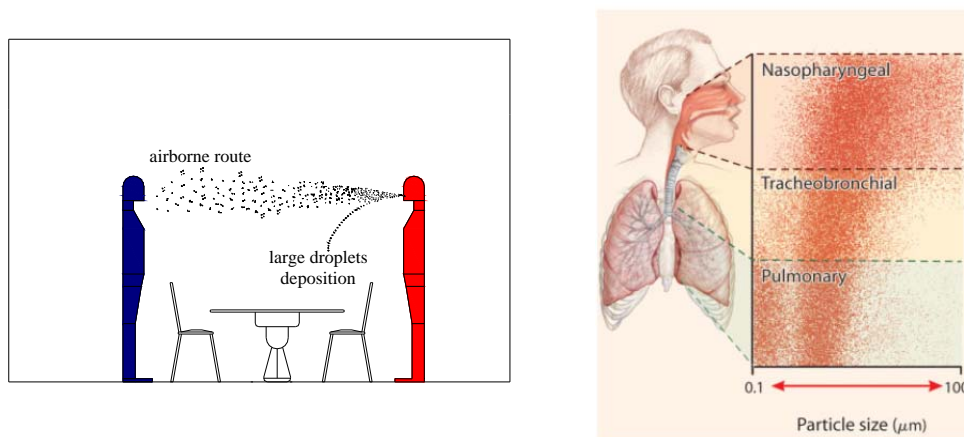


Figure 1.8 a) Dispersion of exhaled particles in a room with two people, in red the person exhaling the contaminants and in blue the susceptible person of being infected, b) Relation between the particles size and the region of the human respiratory system that the particles can reach (Yang et al., 2011)

In order to understand the origin of these fine contaminated exhaled particles, much research has been made. It is known that the exhaled contaminated aerosol contains a large amount of water (Effros et al., 2002), which is partly evaporated when the aerosols are dispersed in the air (Wells 1934). Then the large droplets generated by normal human breathing (Schwarz et al., 2010), coughing or sneezing can become “droplet nuclei” in less than a second (Wan and Chao 2007) and be dispersed in the air. These droplet nuclei can also be produced by human respiratory activities (breathing, coughing, sneezing or talking) (Chao et al., 2009; Morawska et al., 2009) and be spread in the air generating a high concentration values of contaminants in some areas of a room and increasing the risk of cross-infection between people.

1.4 The importance of ventilation systems in preventing airborne cross-infections

Several sources of evidence point out to the airborne route as one of the most efficient routes of transmission of diseases (Roy et al., 2004; Yu et al., 2004). The SARS (*Severe Acute Respiratory Syndrome*) occurred in 2003 in China, reopened previous evaluations about the airborne route of communicable respiratory diseases. Some researchers conclude that the airborne dispersion of contaminants may play a significant role in the dispersion of respiratory diseases (Li et al., 2005; Li et al., 2004). After that, much research has been done about the parameters that influence the airborne transmission route and it has been proved that the ventilation systems and airflow patterns are a key factor in the spread of contaminants in the air (Li et al., 2007). Qian and Li, 2010 demonstrated that the placement of the exhaust openings in an isolation room can also have a significant influence on the efficiency of a system in removing large droplets and droplet nuclei. Some authors have reported that this efficiency depends also on the position of the air inlet and outlet, the presence of elements that can influence the ambient, such as furniture, or the air inlet velocity (Woloszyn et al., 2004; Liu et al., 2009; Cheong et al., 2003).

Generally speaking, different ventilation strategies influence the dispersion of contaminants in indoor environments in different ways. While a mixing ventilation system creates a homogeneous distribution of the contaminants, a displacement ventilation system creates different areas, a clean lower zone and a contaminated upper zone. However, the problem of the displacement ventilation system is when the pollutants are injected into the thermally stratified zone (Li et al 2011; Olmedo et al, 2011; Nielsen et al., 2011). Then the contaminants are trapped in a stratified layer and can provoke high contaminant concentration at the height of the breathing. The risk of cross-infection generated in a ventilated space will depend on the level of exhaled contaminants in the breathing area of a susceptible person.

The four following chapters of this thesis establish a relation between the airflow patterns generated by different ventilation strategies and the human exhaled contaminant concentration in a room.

1.5 Layout of the thesis

The thesis has been written in the following chronological order:

Chapter 1 The overview on the problem of cross-infection between people in indoor environments is given in this chapter. It also presents the summary of the papers which are considered within this work.

Chapter 2 Describes the experimental methodology carried out during the experiments. It includes the whole description of the laboratory facilities, measurements devices and manikins.

Chapter 3 Shows and describes the ventilation strategies used during the experiments and the airflow pattern generated by each of the ventilation systems in a room.

Chapter 4 Deals with the relation between the ventilation strategy used in a room and the dispersion of the contaminated exhalation flow of one manikin.

Chapter 5 Addresses experimental results about the risk of cross-infection between two people in a room with different ventilation strategies. It also presents the influence of

the different parameters in this cross-infection risk which can be: separation distance between the manikins or relative positions.

Chapter 6 Provides an abstract of the results achieved in this study.

Paper I Discusses the characteristics of the human exhalation flow through the mouth with three different ventilation strategies: displacement, mixing and natural ventilation.

Paper II Addresses the analysis of the dispersion of exhaled contaminants and the cross-infection risk between two people in a room provided with displacement ventilation.

Paper III Describes the airflow pattern and velocity profile generated by three different diffusers: semi-circular wall mounted displacement diffuser, four ways ceiling diffuser and ceiling mounted textile diffuser.

Paper IV Shows the experimental results of how a thermal plume of a person can affect its personal microenvironment and therefore the air quality that person breathes.

Paper V Discusses the influence of three ventilation strategies on the risk of cross-infection between two people in a room. Key factors that directly affect the risk of exposure to exhaled contaminants, such as: separation distance or relative position between the manikins, are addressed in the paper.

Paper VI Studies the risk of cross-infection generated between two people in a room with a low-impulse vertical ventilation system. Compares the results with the ones obtained by other ventilation systems (Paper V) and gives a complete overview of the influence of the ventilation systems on the airborne transmission of diseases.

Paper VII Describes a CFD simulation of the IEA 2D test considering it as a three dimensional and unsteady problem.

CHAPTER 2

Materials and method

The results of this thesis are mostly based on experimental tests carried out in a full-scale laboratory at Aalborg University. One or two breathing thermal manikins have been used to simulate people in a room and the risk of cross-infection between them. The measurements have been carried out under different ventilation strategies in the room: non-mechanical ventilation, mixing ventilation, displacement ventilation and low-impulse vertical ventilation. This chapter shortly describes the methodology and the laboratory facilities used during the experimental work.

2.1. Experimental materials and facilities

2.1.1 Test room and measurements facilities

All the experimental test are carried out in a full-scale room, 4.10 m (length), 3.20 m (width) and 2.70 m (height) in the laboratory of the Civil Engineering Department at Aalborg University. The four different air distribution strategies used are: non-mechanical ventilation (NV), mixing ventilation (MV), displacement ventilation (DV) and low-impulse vertical ventilation, which generates downward flow (DWF) and upward flow areas (UWF) in the room. For the mixing ventilation case, a four-way square diffuser is mounted in the centre of the ceiling to produce a well-mixed flow field. For the displacement ventilation case, a wall-mounted semicircular diffuser is placed in the middle of the left wall. Two rectangular return openings, 0.30 m (length) and 0.10 m (width) each, are located in the left wall below the ceiling and used in both cases: the mixing and the displacement ventilation cases. For the vertical ventilation system two textile diffusers are placed next to each other in the ceiling of the room. One circular return opening, 0.12 m diameter, is placed in the back wall of the room at 2.6 m from the floor in this case, see figure 2.1.

The air change rate set in all the experiments is 5.6 h^{-1} , which corresponds to a volume flow rate (q_0) of $296 \text{ m}^3/\text{s}$. The ventilation system provides cold air supply at $16 \text{ }^\circ\text{C}$.

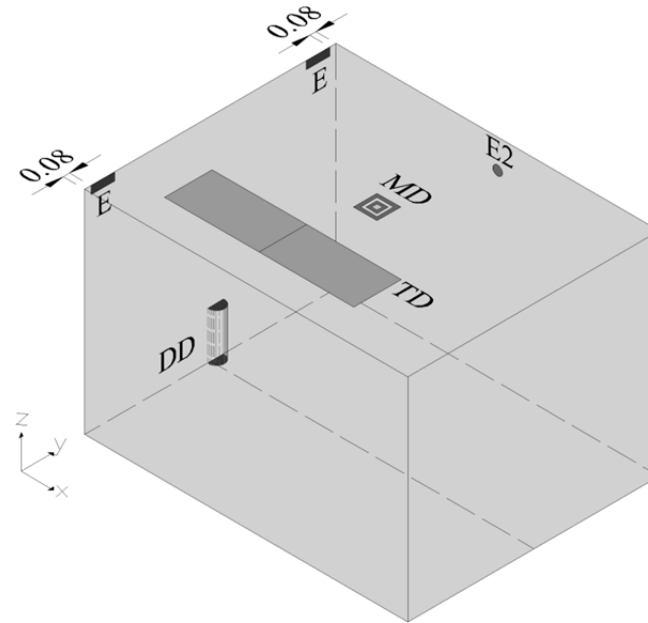


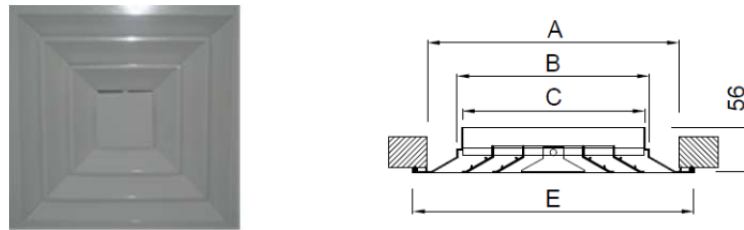
Figure 2.1 Sketch of the test room. Semi-circular displacement diffuser (DD), square mixing diffuser (MD), textile diffusers (TD), return openings for the mixing ventilation and displacement ventilation cases (E), return opening for the vertical ventilation with the textile diffusers (E2)

The test chamber is provided with hot sphere anemometers (Dantec 54R10), which are used to measure air velocity. The air temperature in the test room is measured during all the tests with thermocouples type K and a Squirrel 1000 data logger manufactured by Eltek. A tracer gas, N_2O , is used to simulate exhaled contaminants by one of the manikins in the room. The dispersion of this contaminant is studied and its concentration is measured at several locations with a Multi gas Monitor type 1412 and two Multipoint Sampler and Doser type 1303, both manufactured by Brüel & Kjaer. The accuracy and frequency of each measurement as well as the calibration process of each sensor is explained in Appendix A.

A smoke machine, manufactured by Safex, is also used to visualize the different air flow patterns in the room. An air current test kit used to create smoke to detect the direction of slight air currents in rooms is also used for some of the experiments, e.g.: to visualize the direction of the breathing of the manikins and the flow direction below the diffuser or above the manikins.

2.1.2 Description of the diffusers

The mixing diffuser used to generate a mixing ventilation airflow pattern in the room is a four-way ceiling mounted diffuser; model DSQ 225, manufactured by Madel. Figure 2.2 shows its dimension.



	E	A	C	B
Size (mm)	332	292	212	223

Figure 2.2 Description and size of the four-way ceiling mounted mixing diffuser

For the displacement ventilation cases a semi-circular wall-mounted displacement diffuser is used. The size and dimensions of this diffuser are shown in figure 2.3. The main characteristic is its large supply area that supplies the air into the room at a low velocity.

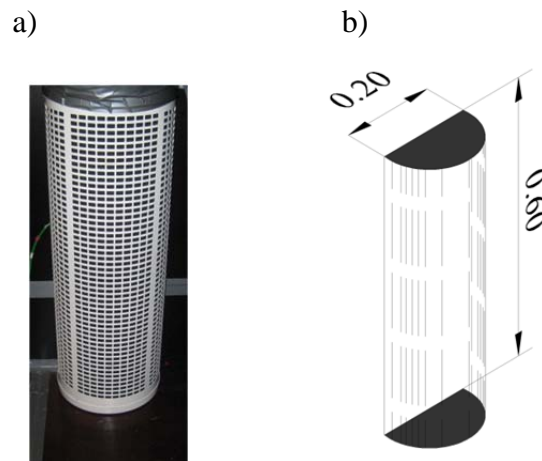


Figure 2.3 Semicircular wall-mounted displacement diffuser a) Picture, b) Size

The low impulse vertical ventilation system consists of two identical textile diffuser placed one next to each other on the ceiling of the room, see figure 2.1. Each diffuser is sized 0.6 m x 1.2 m.

2.1.3 Manikin model of a person

One or two thermal manikins with breathing function are used during the experiments. The manikins are 1.68 m, average-sized women and the total surface area without clothes is about 1.40 m². The manikins have a human body shape in order to be able to accurately simulate the thermal plume generated by a person, see Zukowska et al. (2008). For details

of body shape see figure 2.4. One of the manikins is considered the source, which exhales biological contaminants simulated by the tracer gas N_2O . The target manikin is the one exposed to the exhaled contaminants by the source. With regard to the mouth openings there are slight differences for the two manikins. For the source manikin the mouth has a 123 mm^2 opening and a semi-ellipsoid form and for the target manikin, the mouth consists of a circular opening of diameter of 12 mm. Both manikins exhale the air through the mouth and inhale through the nose. The nose consists of two circular nostrils, with a 6 mm radius each, situated 10 mm above the mouth and facing downwards at a direction of 45° below horizontal plane.

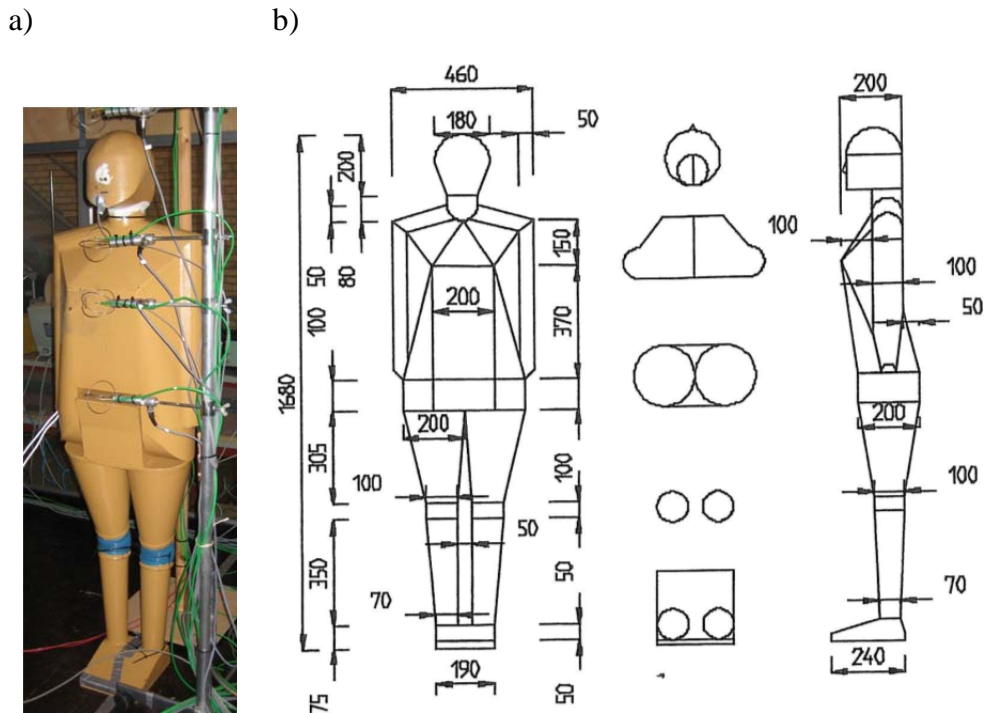


Figure 2.4 a) Picture of the source manikin, b) Detailed description of the manikins' size (Bjørn, 1999)

2.1.4 Simulation of the human breathing

In order to simulate the human breathing two artificial lungs, one for each of the manikins, are used. They can be set to provide a given simulation of the breathing flow with the suitable pulmonary ventilation rate, frequency, gas concentration (in the source manikin) and temperature of the exhaled air. Figure 2.5 shows the two artificial lungs used for the manikins.

The temperature of the exhaled air is kept at $34 \pm 0.5 \text{ }^\circ\text{C}$ using two small heaters mounted in the supply air tubes, which simulate human exhaled air saturated with water vapour at 31°C , see Bjørn (1999). This temperature is corrected in order to compensate for relative humidity in human exhalation.

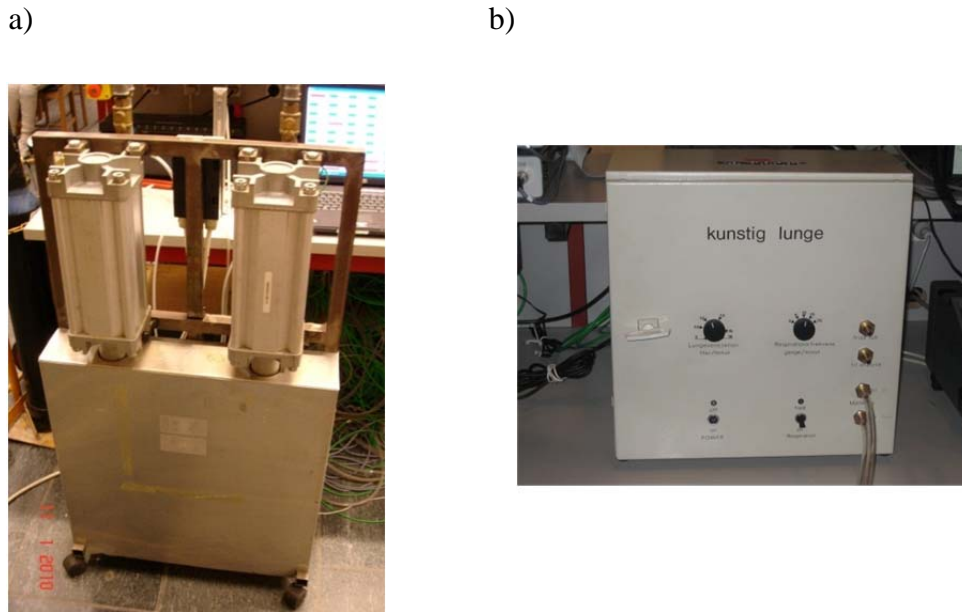


Figure 2.5 Picture of the artificial lungs a) for the source manikin, b) for the target manikin

During the tests, one of the manikins is used as the source manikin. A tracer gas, N_2O , is added to its exhalation in order to simulate small droplet nuclei exhaled by a person that can follow the air stream (Tang et al., 2011). N_2O is commonly known as the “laughing gas”. It is an invisible and odourless gas which has a density similar to air. N_2O is mixed into the supply air in front of the air heater in order to simulate the exhalation of contaminated air from the source manikin. The other manikin is considered the exposed or the target one. Table 2.1 shows the pulmonary ventilation rate simulated for the two manikins for all the tests carried out with the different ventilation strategies.

Table 2.1 Breathing functions of the two manikins for the different ventilation strategies: non-mechanical ventilation (NV), mixing ventilation (MV), displacement ventilation (DV) and low-impulse vertical ventilation placing the manikins in the downward flow area (DWF) and in the upward flow area (UWF)

Ventilation strategy	Source manikin		Target manikin	
	Volume rate (l/exhalation)	Breathing frequency (breaths/minute)	Volume rate (l/exhalation)	Breathing frequency (breaths/minute)
NV	0.57	19.9	0.66	15.0
MV				
DV				
DWF	0.75	14.6	0.66	10.0
UWF				

2.2. Experimental method

2.2.1 Experimental set-up

For all the experimental tests the measurements are taken under steady state conditions. The laboratory where the test room is placed is maintained at a stable temperature similar to the temperature in the test room, in order to minimize the heat fluxes between the test room and the laboratory. Before starting each experiment, the steady state conditions are obtained by using at least five hours to stabilize the temperature in the room. Once the thermal conditions are stable, which means that the temperature in the room is stable at a certain value ± 0.5 °C, the experimental tests were carried out.

The anemometers, thermocouples and concentration tubes are fixed along vertical or horizontal poles placed at different positions in the room.

For the tests to study the airflow patterns in the room, the smoke machine was placed into a wooden box connected to the ventilation ducts.

During the tests where the manikins are used the direction of the exhaled air is to be set horizontally from the mouth using smoke visualisation at the beginning of each experiment.

Each experiment lasts between four and five hours, in order to have enough data to generate reliable average values of velocity, tracer gas concentration and temperature in the room.

2.2.1 Data process

Temperature, velocity and concentration data is measured and recorded. After each experiment the data is post-processed with the corresponding software.

The accuracy of the temperature measurements considering the uncertainties of the probe, wire length and the data acquisition equipment is ± 0.5 °C of the reading. The frequency of the temperature measurements is 30 s.

Velocities are measured with Dantec 54R10 hot sphere anemometers, which are calibrated in a wind tunnel measuring the voltage and the real velocity value using pressure difference values, see Appendix A. The measurements are made with a precision of $\pm 5\%$ at a frequency of 100 ms.

The concentration equipment consists of twelve channels which measure the gas concentration in a sample of air. Measurements are taken for a period of 10 s for each channel consecutively. The accuracy of the concentration measurements is $\pm 1\%$.

The average values during the experiments are used to obtain the thermal, velocity and contaminant concentration conditions in the room for each test.

Instead of the average values, the maximum concentration and velocity values are used to characterize the human breathing exhalation flow, see chapter 4.

CHAPTER 3

Airflow patterns generated in the room

Air diffusers perform in different ways and generate different airflow patterns, temperature and contaminant distributions in a room. Brief descriptions of the airflow pattern generated by three different terminal units: mixing, displacement and a low impulse diffuser are already presented. Smoke visualizations of the airflow and velocity measurements, for each of the terminal units, are also included in order to characterize the diffusers and gain knowledge about the air diffusion that generate in the room. The experimental tests with the wall-mounted displacement diffuser, the ceiling-mounted mixing diffuser and the low impulse textile diffuser were carried out in a full-scale test room at Aalborg University.

3.1 Importance of the air supply conditions

The air movement in a room is controlled or significantly influenced by the air momentum flow produced by the supply opening. Different supply openings generate different airflow patterns and thermal conditions in the room. Therefore, it is important to study the behavior of different diffusers to predict the indoor air conditions in an accurate way.

The correct description of air supply diffusers also plays a crucial role in the CFD predictions of the airflow pattern in a room. Different studies (Lee et al., 2007; Srebric et al., 2008) have demonstrated the importance of the diffuser characteristics and the CFD boundary conditions in the air distribution in a room. In the last years several authors have developed studies regarding different methods of diffuser simulation. The prescribed velocity method (Nielsen, 1997a), the box method (Nielsen, 1997b) and the momentum method (Chen and Moser, 1991) are practical methods for an accurate description of the terminal units in CFD. All of them require some previous experimental measurements to characterize the airflow provided by the diffuser and have been validated by several authors (Koskela, 2004; Huo et al 2000; Einberg et al., 2005; Srebric and Chen 2002).

The main purpose of this chapter is to provide some useful data about the airflow pattern generated by different diffusers, their symmetry or asymmetry, impact on the room conditions and developed regions of the jets. The results will provide knowledge about the airflow patterns generated in a room when the airflow is not influenced by any heat loads and it will provide also valuable information for the validation of CFD simulation methods.

3.2 Materials and methods

Three experimental tests were carried out in a full-scale test room with the internal dimensions of 4.1 m (length), 3.2 m (width) and 2.7 m (height). Figure 3.1(a) shows a sketch of the room with the three diffusers used: a four-way mixing diffuser, a wall-mounted semicircular displacement diffuser and a ceiling-mounted textile diffuser. Only one diffuser was used in each test. In order to create non-isothermal conditions in the room a radiator was also placed in the room. The heat load released was 394 W for all the tests. The position of the diffusers and the radiator in the room is illustrated in figure 3.1(b).

For the tests with the displacement and mixing diffusers two exhaust openings sized 0.3 x 0.1 m and placed in the left wall close to the ceiling were used. For the test with the textile diffuser, a circular exhaust opening (12 cm diameter) is used and placed in the back wall of the room, see figure 3.1. The air exchange rate was set to 5.6 h^{-1} . The details of the size and geometry of the diffusers can be found in chapter 2.

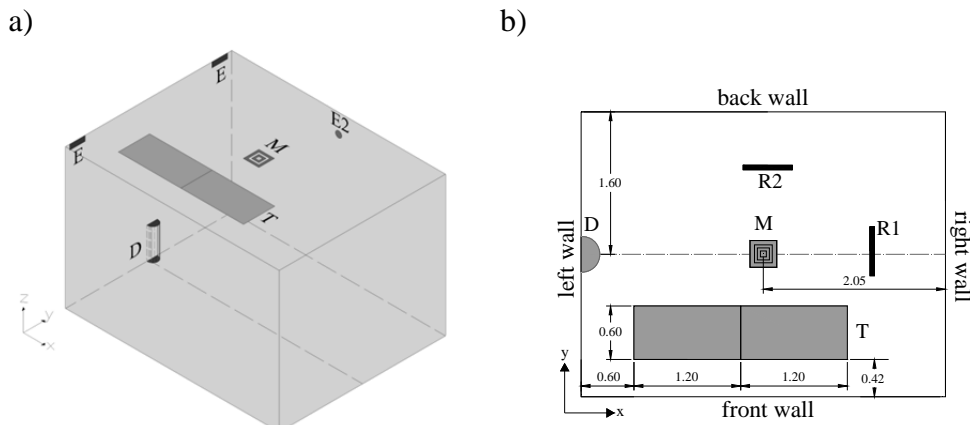


Figure 3.1 a) Sketch of the test room and location of the diffusers and exhaust (D, displacement diffuser; M, mixing diffuser; T, textile diffuser; E, exhaust openings for the mixing and displacement ventilation tests; E2, exhaust opening used with the textile diffuser), b) Placement of the diffusers and radiator in the room (R1, position of the radiator for the tests with the mixing and displacement diffuser; R2, position of the radiator for the test with the textile diffuser)

3.3 Airflow pattern for the mixing diffuser

The flow generated by a mixing ventilation diffuser is mainly controlled by its momentum flow. This section analyses the flow generated by a four-way ceiling mounted diffuser and describes the characteristic equation of the jet generated.

3.3.1 Turbulent isothermal free jets

The air supplied by a mixing diffuser generates a turbulent jet. This jet flows entraining the air in the room and generates a strong mixing process. The velocity of an air jet decreases with the distance to the diffuser. It is possible to describe a line of maximum velocity, which is also called centreline of the jet. Figure 3.2 shows the four regions in which a turbulent jet can be divided:

- ✓ Initial region or velocity core is a short zone. The maximum velocity of the jet remains practically unchanged.
- ✓ Transition region. Its length depends upon the diffuser type. The centreline of the jet is predictable and it is possible to find a relation between the maximum velocity and the distance from the diffuser.
- ✓ Main region: A fully turbulent flow has been established. It is possible to determine the velocity at the centreline of the jet with its characteristic equation.
- ✓ Terminal region: A region far from the diffuser. The initial velocity core is mixed with the surrounding air.

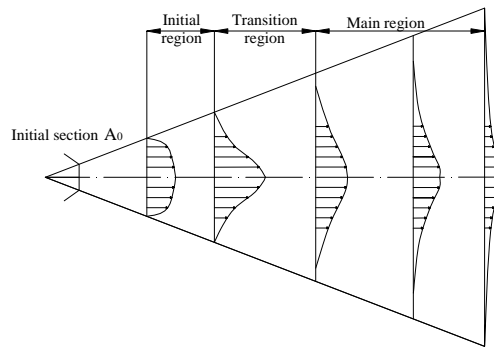


Figure 3.2 Picture of an isothermal jet

The centreline velocity decay of a three dimensional jet can be described by equation (3.1).

$$\frac{u_x}{u_o} = K_v \cdot \left(\frac{x}{\sqrt{A_o}} \right)^{n_1} \quad (3.1)$$

where u_x is the velocity in the centreline, u_o is the velocity at the discharge, x the distance to the diffuser, A_o the free area of the diffuser, K_v the centreline velocity decay constant and n_1 the negative exponent of the velocity decay, which is close to -1.0.

Equation (3.1) can be illustrated and written in its logarithmic form, where the dimensionless velocity u_x/u_o is represented as a function of the dimensionless distance $x/\sqrt{A_o}$ and where the exponent n_1 corresponds to the slope of the straight line of the graph, see figure 3.3 and equation (3.2).

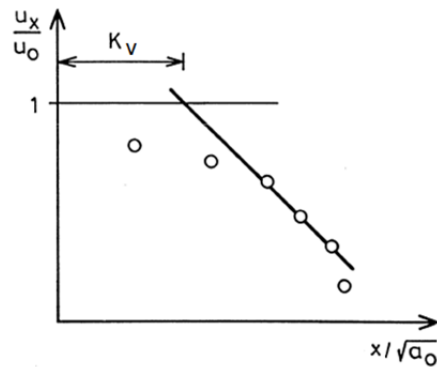


Figure 3.3 Dimensionless velocity versus dimensionless distance for a free jet (Reproduced from Nielsen, 1995)

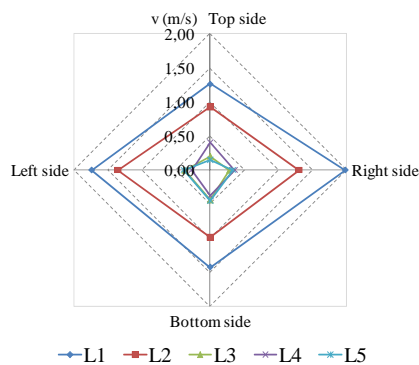
$$\log\left(\frac{u_x}{u_0}\right) = \log K_v - n_1 \log\left(\frac{x}{\sqrt{A_0}}\right) \quad (3.2)$$

A plane wall and free jet will have a slope of -0.5 while a three dimensional wall and free jets will have a slope of -1.0 (Nielsen, 1995).

3.3.2 Airflow and velocity decay

In order to find the velocity profile close to the diffuser at different heights, five hot-sphere anemometers are placed at 0.03 m from the centre of each side of the diffuser. The anemometers are placed at the heights of: 2.65 m, 2.61 m, 2.57 m, 2.53 m and 2.49 m, corresponding with the measurements obtained for L1, L2, L3, L4 and L5 respectively, see figure 3.4(a).

a)



b)



Figure 3.4 a) Velocity profile generated by the ceiling-mounted mixing diffuser, b) Airflow smoke visualization

The velocity profiles obtained shows practically a complete symmetry in the airflow generated by the diffuser at the five heights. However, the results show higher velocity values in the right and left sides of the diffuser, which corresponds to the sides with the largest separation distance from the walls. It may mean a significant influence on the room geometry in the velocity profile

The quasy-symmetry airflow pattern generated by the diffuser is also possible to see with smoke visualization, see figure 3.4(b).

In order to find the characteristic equation of the jet in one of the sides of the diffuser, the vertical line with the five anemometers is moved to 0.53 and 0.83 m from the diffuser on the left side of the diffuser. Figure 3.5 shows the anemometer positions and the velocity profiles obtained at each distance from the diffuser.

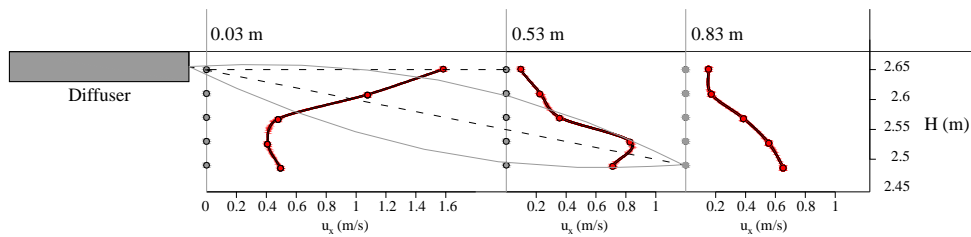


Figure 3.5 Placement of the anemometers respect to the diffuser (grey) and velocity results obtained for each anemometer (red)

For the closest distance, 0.03 m from the diffuser, the maximum velocities are obtained at the heights closest to the ceiling. However, at 0.53 m and 0.83 m from the diffuser the maximum velocities are obtained at the heights of 2.53 and 2.49 m respectively.

The results correspond to the typical developed region of a jet, which entrains the air in the room and disperse the air with a certain angle from the ceiling, which correspond to 15° for this case. The velocity decay of the jet is calculated using the maximum velocity values measured at the separation distances of 0.03 m, 0.53 m and 0.83 m from the diffuser, which corresponds with the anemometers placed at the height of 2.65 m, 2.53 m and 2.49 m respectively.

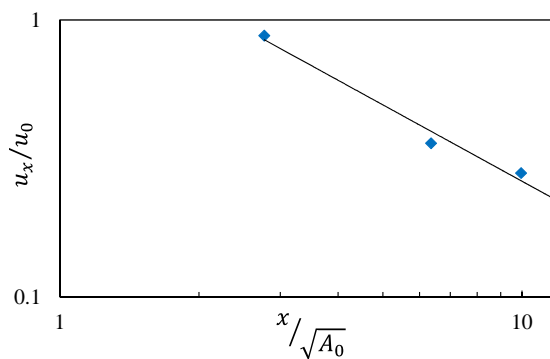


Figure 3.6 Log-log graph representing the velocity decay of the mixing diffuser

Figure 3.6 represents the dimensionless velocity u_x/u_0 as a function of the dimensionless

distance $x/\sqrt{A_0}$ in a log-log graph. The slope of the straight line in the graph represents the velocity decay of the jet, which is -0.92.

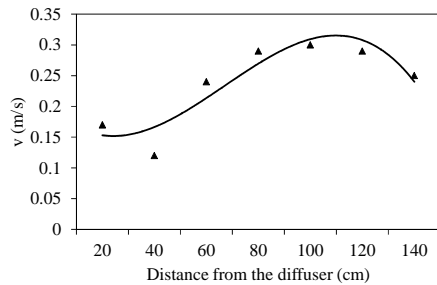
The data of the free opening area of the diffuser is provided by the manufacturer, 0.0227 m², and the maximum velocity, u_0 , is calculated as the division of the volume flow rate, 198 m³/h and the diffuser free area. The value of the constant decay coefficient, K_v , obtained is 2.5, which is a typical value in this kind of diffusers.

3.4 Airflow pattern for the displacement diffuser

The cold air spread at a low velocity in the room by a displacement ventilation system “displaces” the previous air in a room, without producing mixing process. A semi-circular wall mounted displacement diffuser is used to condition the test room and its air flow pattern is measured and visualized with smoke.

Seven anemometers are placed along a horizontal line at 0.01 m height from the floor in order to measure the velocity profile. The horizontal line formed a 45° angle with the center line of the room along the x axis. The first anemometer is placed at 0.20 m from the diffuser and the rest are placed equidistance at 0.20 m from each other.

a)



b)



Figure 3.7 a) Velocity profile generated by the wall-mounted displacement diffuser along at horizontal line at 0.01 m from the floor, b) Airflow smoke visualization

The results show an acceleration of the flow at distances larger than 0.60 m from the diffuser due to the flow of the heavier cold air to the lower part of the room. This velocity is reduced to a value close to 0.20 m/s at 1.40 m from the diffuser, see figure 3.7(a). The stratified and radial flow generated by the cold supply air, which is common with a wall-mounted displacement diffuser (Nielsen, 2000), is shown in figure 3.7(b).

3.5 Airflow pattern for the low-velocity vertical diffuser

In order to measure the velocity profile of a ceiling-mounted low velocity textile diffuser, twelve hot-sphere anemometers are placed along the horizontal line, T1, at 0.80 m from the ceiling, see figure 3.8(a).

The positions of the anemometers in relation to the front wall are shown in table 3.1.

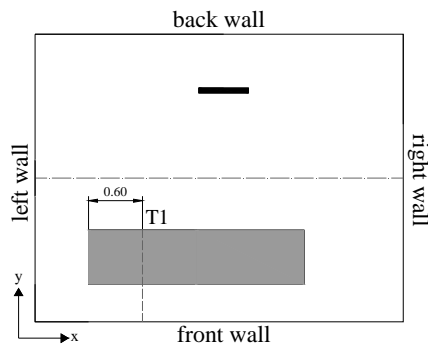
Table 3.1 Position of the anemometers along the horizontal line, T1

Anemometer	y (m)	Anemometer	y (m)
1	0.04	7	0.31
2	0.09	8	0.38
3	0.12	9	0.48
4	0.18	10	0.58
5	0.22	11	0.78
6	0.27	12	0.98

The textile diffuser generates an expected downward flow that is not disturbed by any heat load in the room (the radiator is placed in the opposite side of the room).

The velocity profile measured shows high velocity values in the region close to the wall and lower values in the measurements below the diffuser, see figure 3.8(b).

a)



b)

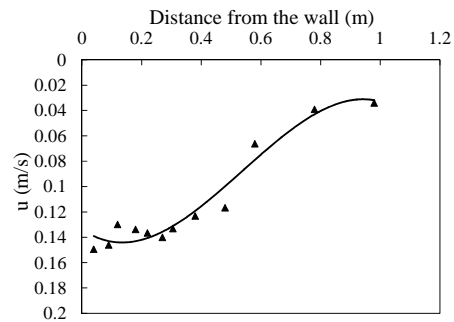


Figure 3.8 a) Placement of the measuring line T1 (diffusers in grey), b) Velocity profile measured at 0.8 m the diffuser along the line T1

This acceleration of the flow close to the wall is due to the Coanda effect generated by the wall, which is also visualized by smoke. Figure 3.9 shows the development of the flow at three different instants of time, where it is possible to notice the tendency of the air to flow to the wall side.



Figure 3.9 Smoke visualization of the flow at three instants of time a) 1s, b) 2.5 s, c) 4.5 s

3.6 Discussion of the results

The results presented show the airflow pattern generated by the different ventilation strategies in the test room. They help us to gain knowledge about the different air characteristics that can be created in a room by the different ventilation systems. This data will be useful to understand the indoor environment conditions created in a room by the different ventilation systems when a person or several people are placed in the room. The following chapters will study the influence of these airflow patterns and other parameters on the dispersion of human exhaled contaminants in a room.

CHAPTER 4

Dispersion of human exhaled contaminants in a room

People that occupy a room are not only very significant heat loads but they can also be the most relevant source of biological contaminants, as the human exhaled air can contain different pathogens such as viruses or bacteria. Expiratory droplet nuclei generated by an infected person can spread in the air through the airflow pattern and may increase the pathogen concentration in different indoor environment areas. The purpose of this study is to investigate the influence of the indoor conditions generated by different air distribution strategies on the behaviour and trajectory of the human exhalation flow. It is also the objective to find a possible correlation between the velocity and contaminant concentration of the exhalation flow and its trajectory. This chapter will also analyse the influence of the thermal plume generated by a manikin, simulating a standing person, in the air quality that this manikin breathes. Papers I, IV and VI address the results of this chapter.

4.1 Experimental conditions in the room with one manikin

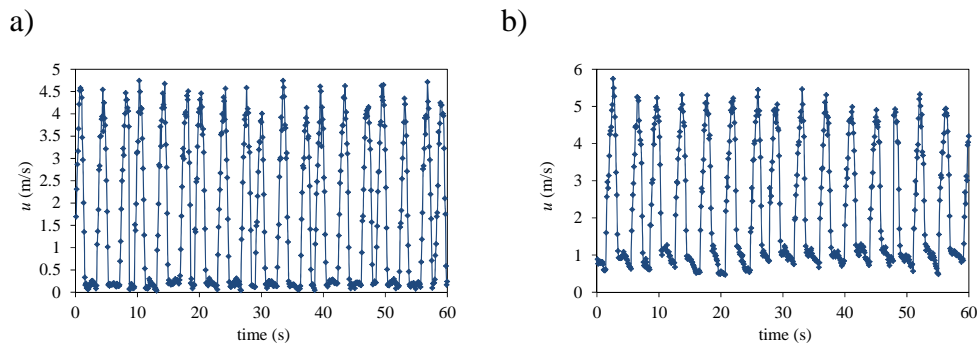
A breathing thermal manikin is used to simulate a standing person in a room, which is conditioned by different ventilation strategies: non-mechanical ventilation (NV), mixing ventilation (MV), displacement ventilation (DV), and low-velocity vertical ventilation, which generates downward flow (DWF) and upward flow (UWF) areas in the room.

The manikin inhales through the nose and exhales through the mouth. The temperature of the exhalation flow is set at 34°C for all the tests. A tracer gas, N₂O, is added to the exhalation flow in order to simulate small exhaled particles as its distribution in the air is identical to the distribution of droplet nuclei (Tang et al., 2011; Yin et al., 2011).

For the different ventilation systems used, the breathing function of the manikin changes as is shown in table 4.1. Figure 4.1 shows the velocity measurements of the exhalation at the mouth of the manikin for the two different breathing functions used. During the time that the exhalation has a velocity close to zero the manikin is inhaling through the nose. The resulting breathing function of the manikin is quite similar to the normal breathing of a person and is considered a sinusoidal function of time (Gupta et al., 2010).

Table 4.1 Breathing functions of the source manikin

		SOURCE MANIKIN		
		Volume rate (l/exhalation)	Breathing frequency (breaths /minute)	Maximum velocity (m/s)
Group A	NV	0.57	19.0	4.74
	MV			
	DV			
Group B	DWF	0.75	14.6	5.76
	UWF			

Figure 4.1 Exhalation velocity profiles for the two groups of cases. a) *Group A*, b) *Group B*

For the experiments, the source manikin is used to investigate the influence of different ventilation strategies on the behaviour of the exhalation flow. Different ventilation strategies produce different airflow patterns, temperature distribution and therefore different temperature differences between the exhalation flow and the surrounding air. These facts can directly affect the direction, trajectory and distance that the exhalation jet flows. The penetration distance of this contaminated flow is a crucial factor in order to study the risk of cross-infection in a room when it is occupied by several people.

The experimental work to study the exhalation flow under different ventilation strategies consists of five tests. Table 4.3 shows a sketch of each of the cases studied. For the tests, the standing thermal breathing manikin is placed in the room together with a radiator. The heat load released by the manikin is 94W while the radiator is responsible for 394 W. The position of the manikin and the radiator for each case, as well as the measuring lines used to place the sensors, are shown in figure 4.2.

Additionally, for the displacement ventilation case, the influence of the thermal plume on the air quality that the manikin breathes is also studied. In this case the source manikin is operated under three different heat fluxes; corresponding with different surface temperatures, in order to study the thermal plume generated by different metabolic rates, see table 4.2. The heat load of the radiator is maintained at 394 W.

Table 4.2 Heat load released by the manikin for the study of the thermal plume

SOURCE MANIKIN	
Heat load (W)	Surface temperature (°C)
0	-
94	29.9
120	31.0

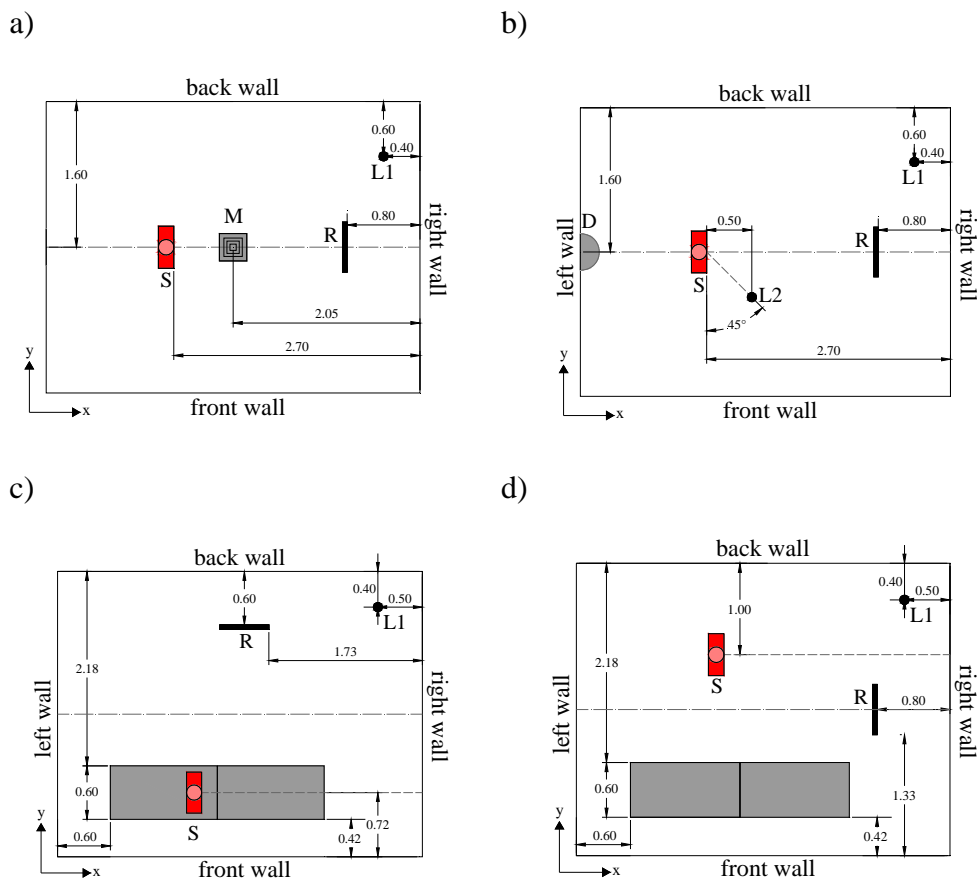
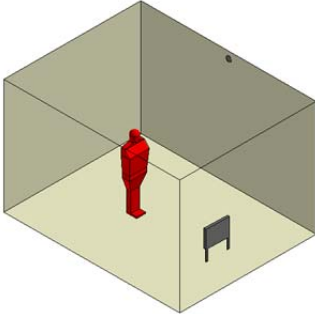
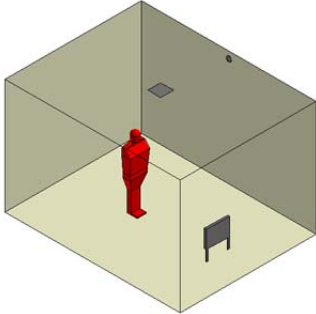
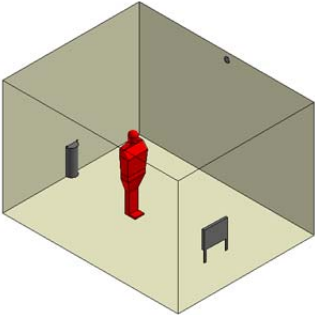
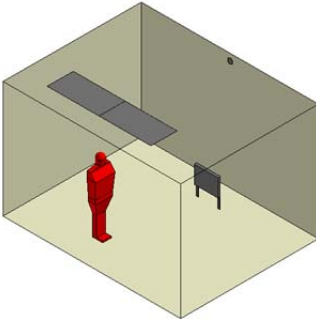
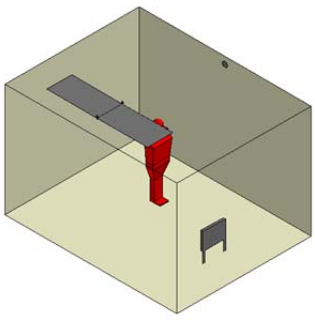


Figure 4.2 Placement of the source manikin (S), radiator (R), vertical lines, L1 and L2 and diffusers a) Mixing ventilation (M) and without mechanical ventilation, b) Displacement ventilation (D), c) Vertical ventilation with the textile diffuser (T) for the downward flow position, d) Vertical ventilation with the textile diffuser (T) for the upward flow position

Table 4.3 Position of the manikin with the different ventilation strategies

GROUP A		
Non-mechanical ventilation	Mixing ventilation	Displacement ventilation
		
GROUP B		
Low-velocity vertical ventilation		
Downward flow	Upward flow	
		

4.2 Influence of the thermal plume on the air quality a person breathes

This part of the chapter will investigate the PME (*Personal Micro Environment*) of the manikin under displacement ventilation conditions. The aim is to increase the knowledge of how the thermal plume generated by a person affects the PME and therefore the concentration of contaminants in the inhalation area.

An experimental study in the room with the displacement ventilation system is carried out. The convective transport mechanism, which is found in the thermal plume around a person, influences the human exposure to pollutants in this environment (Murakami, 2004).

In this case the source manikin is operated in three different heat fluxes; see table 4.2, to simulate different metabolic rates.

During the experiments ten concentration probes were placed in the room. Three concentration tubes were fixed to the surface of the manikin at three different heights: hips (0.95 m), chest (1.25 m) and nose (1.53 m in the inhalation tube of the manikin). The other seven tubes were situated along the vertical lines L1 and L2, four along L1 at the heights of 0.05 m, 1.25 m, 1.80 m and 2.15 m and three in L2 at the heights of 0.95 m, 1.25 m and 1.53 m, see figure 4.2(b).

Figure 4.3 shows the vertical contaminant distribution in the room along L1 and L2. The results show a strong vertical contaminant gradient typical of a displacement ventilation system along the two vertical lines. For L1, the contaminant distribution is almost the same for the three heat loads used. However, for L2 the contaminant concentration increases with the heat load released from the manikin.

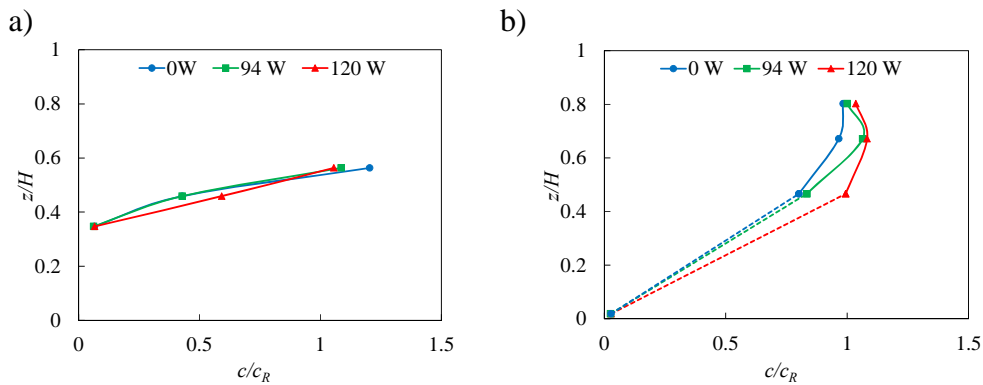


Figure 4.3 Concentration values along the vertical lines using the displacement ventilation strategy. a) L1 in the room, b) L2 at 0.50 m from the manikin

The contaminant concentration in the surface of the manikin at three different heights, the hips, the chest and the inhalation through the nose are show in figure 4.4.

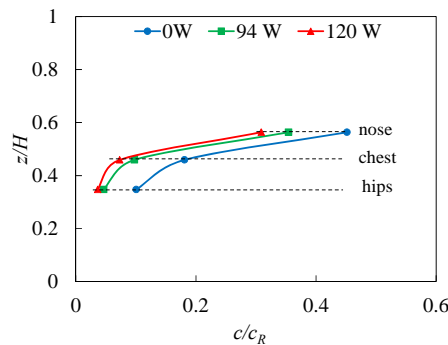


Figure 4.4 Concentration values in the thermal plume of the manikin at the height of the hips, chest and in the inhalation using the displacement ventilation strategy

The three cases considered 0 W, 94 W and 120 W, show a similar shape of the contaminant

concentration profile where the highest amount of contaminants is in the inhalation area. This is due to the typical distribution of contaminants in a displacement ventilated room where the lower area is maintained cleaner than the upper area of the room; see figure 4.3.

The air inhaled by a manikin comes from the lower part of the room, due to the convective flows, (Hayashi et al., 2002, Zhu et al., 2005, Murakami, 2004). A strong thermal plume induces more clean air from the lower area of the room that flows upwards to the inhalation area. In consequence, the higher the heat flux is the lower the concentration of contaminants is in the inhalation area.

4.3 Study of the exhalation flow

In this section, the main objective of the experimental tests, *Groups A and B*, is to observe and determine the centreline of the exhalation flow under different ventilation strategies in the room, considering the exhalation as a non-isothermal jet. After this, it is possible to relate the trajectory of the exhalation jet with the maximum velocity and concentration values measured along the centreline.

4.3.1 Thermal conditions in the room

The environmental conditions created by the different ventilation systems in the room can directly affect the trajectory of the exhalation flow. In each of the cases studied one vertical line, L1, with five thermocouples placed at the heights of: 0.1 m, 0.6 m, 1.1 m, 1.8 m and 2.1 m, is located in the room, see figure 4.2. The vertical temperature distributions found for the displacement ventilation, mixing ventilation and vertical ventilation cases are shown in figure 4.5.

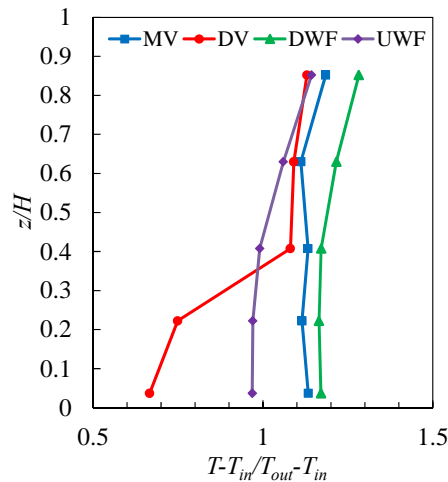


Figure 4.5 Vertical temperature distributions in the room along L1 for the four cases with mechanical ventilation

It is possible to see the typical vertical temperature stratification for the displacement ventilation case. For the mixing ventilation case the temperature values are very close to 1.0, which means that the air is fully mixed in the room. The temperature level for the cases of vertical ventilation, DWF and UWF, is slightly higher than in the other two cases and shows a constant temperature level close to 1.0 as was measured in the mixing ventilation case.

4.3.2 Centreline of the exhalation flow

The exhalation flow can be described as a non-isothermal jet. In this way, the exhalation jet will entrain the air in the room increasing the width of the jet as the distance from the mouth increases. However, the penetration length of the exhalation flow can vary with the different ambient conditions created in the room. During these tests, five gas samplers and five anemometers are used to measure the concentration and velocity in the exhalation flow of the breathing. The sensors are situated along the centreline of the exhalation flow in order to measure the peak centreline values. These five positions are found visualizing the exhalation flow with smoke, see figure 4.6. Five anemometers are placed along the visualized centreline to measure the instantaneous velocity. After placing the anemometers, smoke is used to confirm that their positions correspond to the centreline of the exhalation airflow previously visualized. This process is repeated until the five positions along the centreline are found.

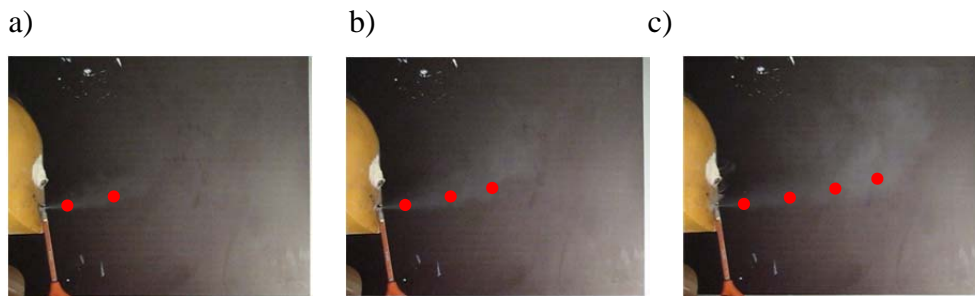


Figure 4.6 Smoke visualization of the exhalation jet in the displacement ventilation case and placement of the probes along the centreline at different time intervals a) 0.1 s, b) 0.3 s and c) 0.55 s

During the experiments special care was taken to find the best position of the manikin to generate a horizontal airflow exhalation. Figure 4.6 illustrates the visualization of the jet with smoke in order to find the centreline of the exhalation at different instants of time. It is important to notice that the further the probes are from the mouth the more the velocity of the exhalation jet is affected by the turbulence. This fact makes the process of finding the centreline of the jet more difficult at further distances from the mouth.

The positions of the anemometers and concentration tubes placed to take measurements along the centreline of the exhalation flow for each case: non-mechanical ventilation (NV), mixing ventilation (MV), displacement ventilation (DV) and vertical ventilation, downward (DWF) and upward (UWF) positions, are shown in figure 4.7. The position of each sensor in the room is given in table 4.4.

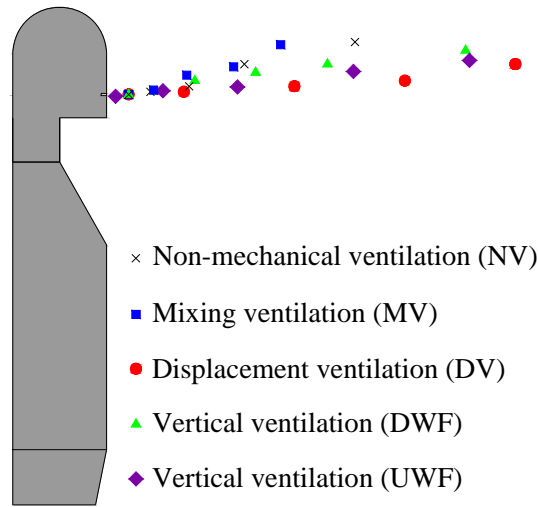


Figure 4.7 Placement of the anemometers and concentration tubes along the centreline of the exhalation flow respect to the manikin for each case studied

Table 4.4 Position of the anemometers and concentration tubes along the centreline of the exhalation flow

		Non-mechanical ventilation (NV)				
Horizontal distance (m)		0.04	0.08	0.15	0.25	0.45
Height (m)		1.52	1.525	1.535	1.575	1.615
		Mixing ventilation (MV)				
Horizontal distance (m)		0.04	0.085	0.145	0.23	0.315
Height (m)		1.52	1.528	1.55	1.57	1.61
		Displacement ventilation (DV)				
Horizontal distance (m)		0.04	0.14	0.34	0.54	0.74
Height (m)		1.52	1.525	1.535	1.545	1.575
		Vertical ventilation (DWF)				
Horizontal distance (m)		0.04	0.16	0.27	0.40	0.65
Height (m)		1.525	1.545	1.56	1.575	1.60
		Vertical ventilation (UWF)				
Horizontal distance (m)		0.01	0.095	0.23	0.44	0.65
Height (m)		1.52	1.53	1.537	1.565	1.585

4.3.3 Airflow model of exhalation flows

Considering the human exhalation flow as an instantaneous non-isothermal turbulent jet, it is possible to relate its trajectory with other characteristic parameters by an equation similar to the one proposed by Baturin (1972) for steady state flow. The theory of the non-isothermal jets describes their centreline as curved. Looking at the velocity and

concentration probes positions to find the centreline of the exhalation jet, figure 4.7, it is possible to observe the different curved trajectories obtained for the different ventilation strategies, see figure 4.8.

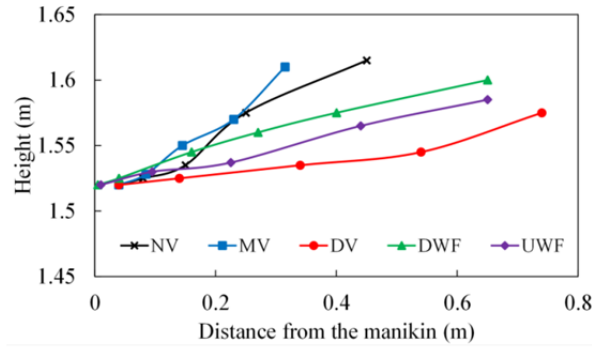


Figure 4.8 Centreline of the exhalation jets for the five ventilation principles

The Archimedes number is used to measure the motion due to density difference. Considering the exhalation flow as a non-isothermal jet with a temperature T_0 different from the temperature in the room, T_{amb} , the buoyancy can directly affect the exhalation flow. It is possible to characterize the exhalation flow by the following Archimedes number:

$$Ar = \frac{\beta g \Delta T \sqrt{a_0}}{u_0^2} \quad (4.1)$$

where β , g , a_0 , u_0 and ΔT are volume expansion coefficient, gravitational acceleration, mouth opening surface (123 mm²), maximum velocity of the exhalation flow and temperature difference between the exhalation flow, T_0 , and the ambience in the room, T_{amb} . T_{amb} is obtained as the average value of two temperature values given by two thermocouples placed 1.3 m and 1.7 m height at 0.40 m from the manikin.

Table 4.5 shows the temperature of the surroundings of the exhalation flow, T_{amb} , the temperature difference, ΔT , with the exhalation airflow temperature, T_0 , and the corresponding Ar number obtained.

For the displacement ventilation case, the Ar number obtained is lower than for the other two cases with the same breathing function, mixing ventilation and the case without mechanical ventilation. It means that the strength of free convection is larger for the displacement ventilation case and therefore the exhalation jet projects less upward. This fact is directly related with the temperature difference, ΔT , which shows the lowest value for the displacement ventilation case. For this case, the vertical temperature stratification maintains the temperature at the height of the exhalation higher than in the rest of cases. This fact produces a lower temperature difference with the exhalation flow. The stable temperature layer generated by the displacement ventilation system at the height of the breathing maintains the exhalation flow more stable and reduces the mixing process of the exhalation flow with the surrounding air. It can make difficult for the exhalation flow to project to the upper part of the room and to entrain the surrounding air reducing the

contaminant concentration. This phenomenon will provoke a higher contaminant concentration around the height of the breathing (Bjørn and Nielsen, 2003; Li et al., 2011).

Table 4.5 Temperature data obtained for the five ventilation strategies, $T_0=34$ °C

Ventilation strategy	T_{amb} (°C)	ΔT ($T_0 - T_{amb}$)	$Ar * 10^7$
Non-mechanical ventilation (NV)	22.8	11.2	9.6
Mixing ventilation (MV)	22.9	11.1	9.5
Displacement ventilation (DV)	23.6	10.4	8.9
Vertical ventilation (DWF)	22.3	11.1	6.8
Vertical ventilation (UWF)	22.9	10.7	6.5

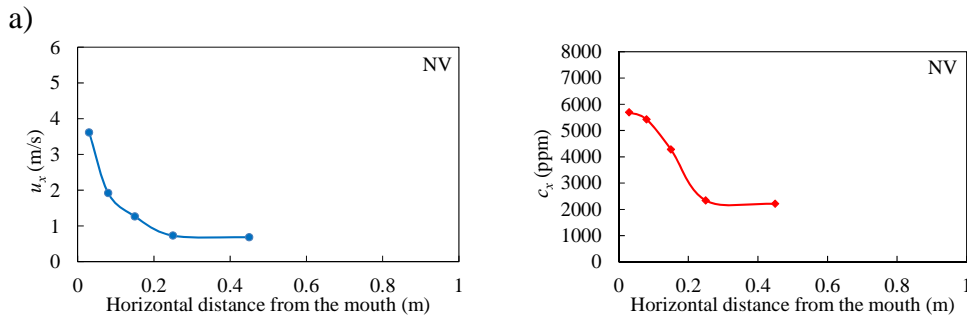
For the mixing ventilation and without mechanical ventilation cases, the exhalation jets flow upper than in the displacement case and shows higher Ar numbers and temperature difference, ΔT . The exhalation jets are nearly the same for the two cases (with mixing and non-mechanical ventilation) which agrees with the results obtained by Liu et al., 2009.

For the vertical ventilation cases, the Ar number obtained are lower than in the displacement ventilation because of the larger value of the velocity inlet of the breathing. However, the trajectories of the exhalation jets flow slightly more upward than in the displacement ventilation case due to the higher temperature difference, ΔT .

Therefore, the penetration distance is directly affected by the temperature conditions in the surroundings of the manikin that are created by the different ventilation strategies. It is especially important the microenvironment generated around the thermal manikin since the surrounding air temperature influences the convective transport and can make the exhalation flow in different directions.

4.3.4 Velocity and concentration decay

The maximum velocity and concentration decays of the exhalation jet for each case are shown in figure 4.9. The maximum velocities at each point of the centreline are obtained as the average values of the maximum velocity values measured in the breathing during each experiment. For the concentration decay the maximum concentration value obtained during the measurements is used. The maximum velocity and concentration values along the centreline, u_x and c_x , are given as a function of the distance to the manikin's mouth.



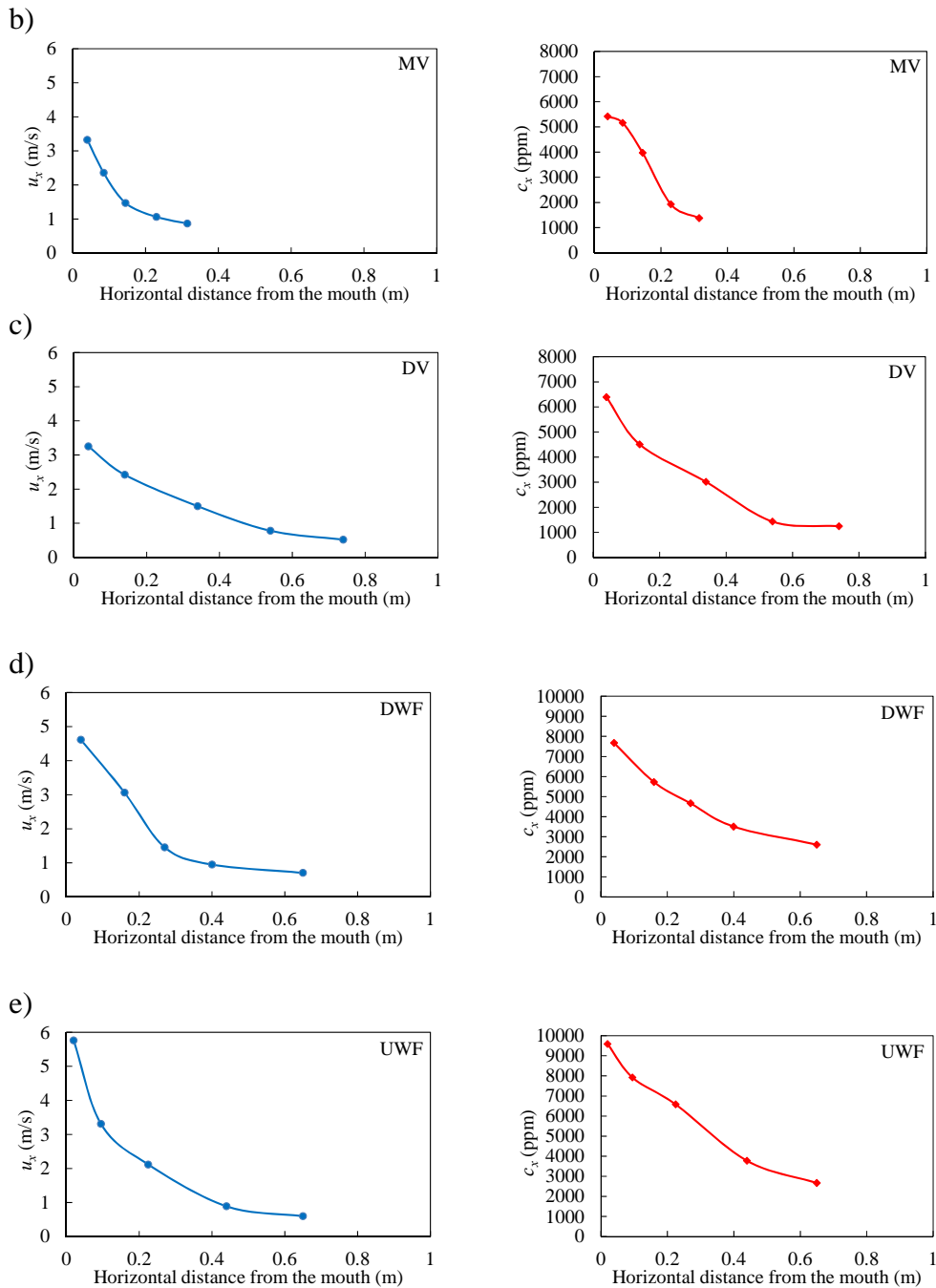


Figure 4.9 Velocity and concentration decay of the exhalation jet for the five cases studied. a) Non-mechanical ventilation, b) Mixing ventilation, c) Displacement ventilation, d) Vertical ventilation in the downward flow area, e) Vertical ventilation in the upward flow area

Nielsen et al. (2009) have shown that peak values for exhalation velocity of the instantaneous human exhalation flow can be described by an expression where the peak velocity is a linear function of the reciprocal horizontal distance from the mouth. This relation is expressed by the following equation, similar to the expression for the centreline velocity in a free jet:

$$\frac{u_x}{u_o} = K_{exp} \cdot \left(\frac{x}{\sqrt{a_o}} \right)^{n_1} \quad (4.2)$$

where K_{exp} is a characteristic constant, a_o the area of the mouth, x the horizontal distance from the mouth where the measurements are taken, and u_x and u_o are the peak values of the velocity at distance x and in the mouth respectively. For the cases of Group A and B, the velocity values measured at the manikin's mouth are 4.74 m/s and 5.76 m/s, respectively.

In the same way, peak concentration values of the samples measured during breathing are also related to positions, as shown in the following equation:

$$\frac{c_x - c_s}{c_o - c_s} = K_c \cdot \left(\frac{x}{\sqrt{a_o}} \right)^{n_2} \quad (4.3)$$

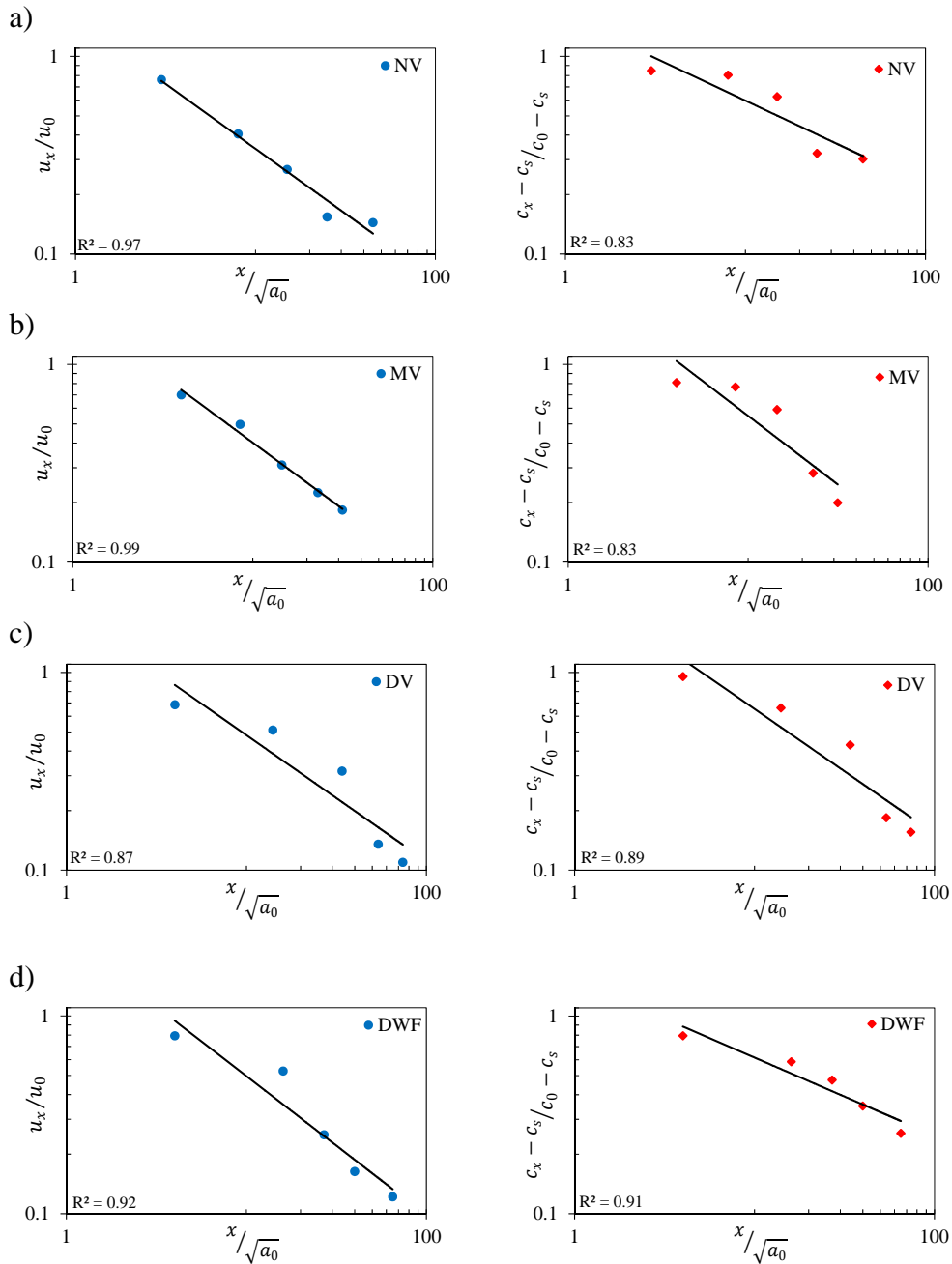
where K_c is a characteristic constant and c_x , c_o and c_s are peak concentration values measured at a horizontal distance x from the mouth, in the mouth and in the surroundings, respectively. The values of c_s are measured at the chest of the manikin. It is important to point out that the measured peak concentration is influenced by the measuring equipment where some averaging takes place. The concentration values at the mouth for the tests of Groups A and B are 6687 ppm and 9599 ppm, respectively.

The values of the characteristic constants and exponents, for the five cases studied, are shown in table 4.6.

Table 4.6 Characteristic velocity and concentration constants and exponents for the exhalation jets

Ventilation strategy	c_s (ppm)	K_{exp}	n_1	K_c	n_2
Non-mechanical ventilation (NV)	262	4.5	-0.66	8.5	-0.43
Mixing ventilation (MV)	47	4.5	-0.68	6.3	-0.69
Displacement ventilation (DV)	58	7.5	-0.64	10.8	-0.63
Vertical ventilation (DWF)	208	6.6	-0.70	11.6	-0.39
Vertical ventilation (UWF)	206	5.8	-0.64	12.1	-0.36

Figure 4.10 is the graphic representation of the equations (4.2) and (4.3) for the exhalation flow with the five air distribution principles. The dimensionless velocity u_x/u_o and concentration $c_x - c_s / c_o - c_s$ are shown as a function of the dimensionless distance x/a_o in a log-log graph.



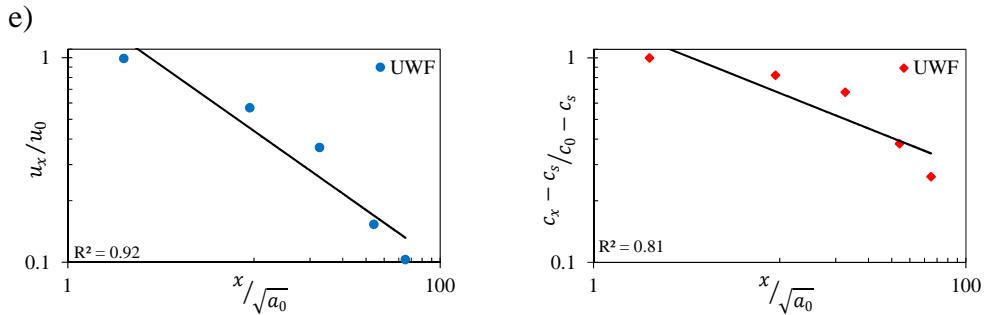


Figure 4.10 Velocity and concentration level along the centreline of the exhalation jet versus distance to the mouth in a log-log graph for the different ventilation strategies. a) non-mechanical ventilation, b) mixing ventilation, c) displacement ventilation, d) vertical ventilation with downward flow, e) vertical ventilation with upward flow

Finally, figure 4.11 compares the velocity and concentration decays obtained for the five cases studied in a log-log graph. For the velocity results, figure 4.11(a), it is possible to observe a very similar slope, in all the cases with a numeric value close to -0.65. This value is not very different from -0.5, the slope obtained for a plane free jet. However, the concentration results are less homogenous and the slope varies from case to case, see figure 4.11(b).

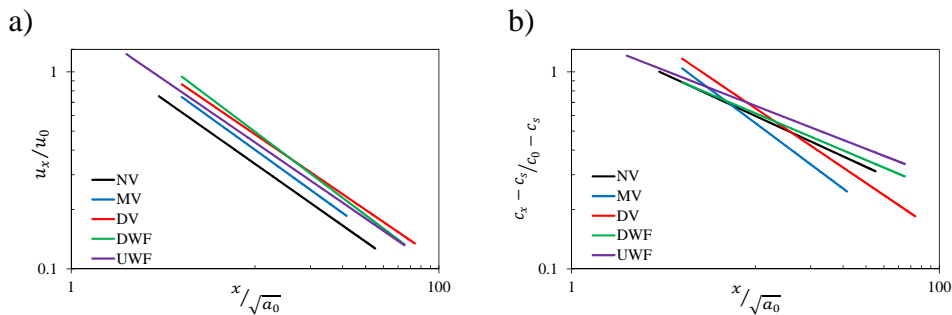


Figure 4.11 a) Comparison of the velocity decay in a log-log graph, b) Comparison of the concentration decay in a log-log graph

4.4 Conclusions

The results show that the thermal plume generated by a person influences the air quality in the breathing area. For the displacement ventilation case studied, the higher heat load released by the manikin, the higher amount of air is induced to the inhalation area by the thermal plume. Therefore the lower contaminant concentration is found in the breathing area because the displacement ventilation works with two zones in the room, a clean lower area and a contaminated upper area.

Different ventilation systems create different airflow patterns and different temperature distributions in a room. The temperature difference between the exhalation flow and the ambience directly affects the direction and penetration length of the exhalation flow. Using the same initial velocity of the breathing, the larger the temperature difference between the exhalation and the surrounding air is, the more upward the jet flows.

The maximum velocity decay and the maximum average concentration decay in the exhalation can be described by simple expressions that show the variables as proportional to the reciprocal horizontal distance from the mouth.

CHAPTER 5

Cross-infection between people in a room

When several people are placed in the same room the dispersion of exhaled contaminants can produce a risk of cross-infection between people. An infectious person can exhale airborne pollutants that are spread in the air. A susceptible healthy person placed in the same room may be exposed in a higher or lower level to the exhaled contaminants. This level of exposure depends not only on the air distribution system but also on people's different positions, the distance between them, direction of exhalation and surrounding temperature and temperature gradient. In this chapter experimental measurements using two breathing thermal manikins and four different ventilation strategies are carried out. The main objective of this chapter is to study the key factors in indoor environments that may affect the exposure level to contaminants and therefore the risk of cross-infection. All the results are addressed in paper V and paper VI.

5.1 Evidences of cross-infection risk in indoor environments

In recent years, an interest in understanding the mechanism of airborne infection between people in the same room has increased significantly. Several studies have shown evidence that relate the ventilation systems with the distribution of contaminants and airborne transmission of diseases in rooms (Li et al., 2005; Li et al., 2007; He et al., 2005; Mui et al., 2009); Richmond-Bryant, 2009). Displacement ventilation system was supposed to be a very efficient system producing a clean area in the breathing zone of the room (He et al., 2005) and preventing the risk of cross-infection between people in a room (Gao and Niu, 2006). However, the temperature gradient may, on the other hand, result in high concentration at different heights, e.g. the breathing zone as shown by Bjørn and Nielsen (2002) and Qian et al. (2006), causing a reduced protection against the exposure to contaminants. On the other hand, Nielsen et al. (2008) showed that full mixing of the air can limit the concentration of the pollutants in the breathing zone of the exposed person. However, there are a lot of key factors that may influence the efficiency of the ventilation systems in removing contaminants in a room. Location of the exhaust and supply openings is one of the factors that directly affect the dispersion of contaminants in indoor environments. Some authors determined the influence of these factors in the spread of

contaminants in hospital wards (Nielsen, 2009; Chung and Hsu, 2001; Qian et al., 2008; Nielsen et al., 2010; Lim et al., 2010) and isolation rooms (Cheong and Phua, 2006). Woloszyn et al., 2004 also concluded that the presence of obstacles in a room will condition the airflow pattern and the contaminant distribution in a room. In the same way, the position of thermal loads and people in a room also influence the airflow patterns (Liu et al., 2009; Lee et al., 2005).

The results presented in this chapter show the results of the personal exposure between two manikins in a room with different ventilation strategies and different separation distances and relative positions between the manikins in the room. Paper V and VI address the result of the experiments.

5.2 Methods

For the experimental tests described in this chapter, two breathing thermal manikins are used. One of them is considered the infectious one, the source manikin, and the other is the one exposed to the exhaled contaminants, the target manikin. Both manikins inhale through the nose and exhale through the mouth. It is possible to find a complete description of the breathing cycles of each manikin in Chapter 2. The source manikin exhales the contaminants simulated by a tracer gas, N_2O . It has been proved by several studies (Gao and Niu, 2007; Yin et al., 2011) that the use of tracer gas is a valid way to simulate the small droplets generated by the human breathing.

The thermal conditions in the room are maintained at the same level for all the experimental tests. Each manikin is responsible of 94 W while the radiator placed in the room is responsible of 300 W. The air change rate is set at 5.6 h^{-1} .

The separation distance and relative position between the manikins and respect to the diffusers have been changed in order to gain knowledge about the influence of these key factors on the exposure level.

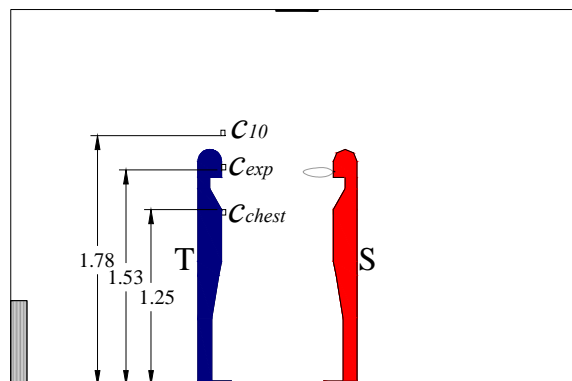


Figure 5.1 Sketch of the test room with the source (S) and the target (T) manikins and location of the concentration tubes at the chest (c_{chest}), the inhalation (c_{exp}) and above the manikin (c_{10}). The separation distance between the manikins in the pictures is 0.80 m. All measurements in meters

The results of the exposure level are shown as dimensionless values of the concentration at

different positions at the target manikin, see figure 5.1: the chest, c_{chest} , the inhalation through the nose, c_{exp} , and 0.1 m above the manikin, c_{10} . The exposure is calculated using the average concentration values in the inhalation of the target manikin divided by the exhaust concentration of the room. Using this expression a higher exposure is equivalent to a higher risk of airborne infection between the contaminated and the exposed person simulated by the source and the target manikins, respectively. This expression for the exposure is called “susceptible exposure index” by Qian and Li (2010). The exposure at the chest and above the head of the target manikin is also calculated using the average concentration at these positions divided by the exhaust concentration of the room, in order to analyze the contaminant exposure in the microenvironment around the manikin.

5.3 Two manikins within a room with displacement ventilation

5.3.1 Layout of the tests

For the tests carried out with the displacement ventilation system different relative positions of the manikins are studied. Four relative positions: face to face, face to back, face to side and with the source manikin seated are studied, see figure 5.2.

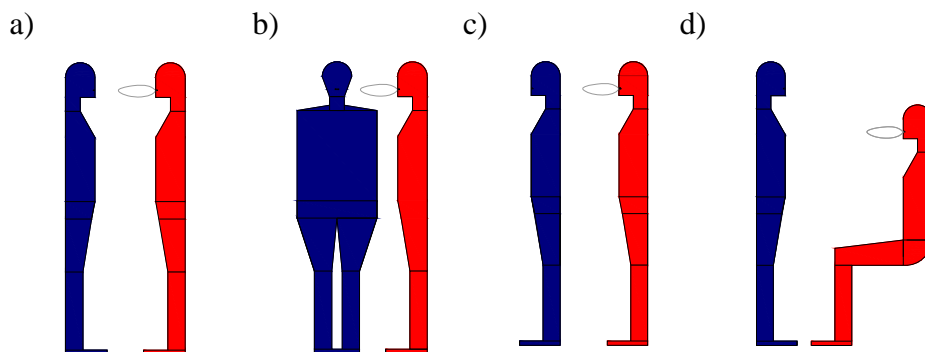


Figure 5.2 Relative positions of the manikins (source in red and target in blue) a) Manikins standing face to face, b) Manikins standing face to side, c) Manikins standing face to back, d) Source manikin seated and target manikin standing

During all the experiments, the manikins are placed along the centreline of the room in the direction of the x axis. The source manikin was always placed at 0.80 m from the radiator and the target manikin was moved to obtain the different separation distances: 0.35 m, 0.50 m, 0.80 m and 1.10 m, see figure 5.3. For the test with the source manikin seated, the position of the source manikin respect to the radiator was the same but the separation distances between the manikins were 0.70 and 1.10 m, owing to the geometry of the manikins. In the case with the target manikin turned 90°, face to side case, the target manikin is facing the back wall and its nose is placed at the same line of the x axis. The vertical temperature distribution in the room was measured with five thermocouples along

the vertical line L1 at the heights of 0.1 m, 0.6 m, 1.1 m, 1.7 m and 2.3 m, see figure 5.3. A summary of the tests carried out is shown in table 5.1.

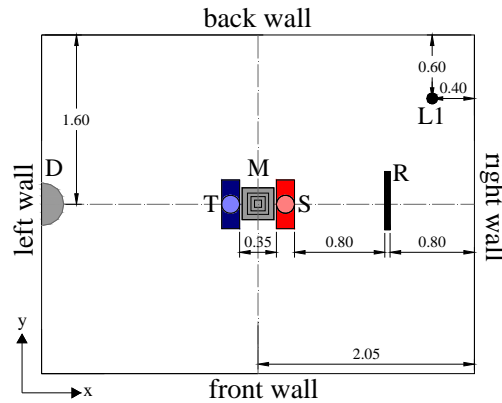


Figure 5.3 Experimental setup with the two manikins (T, target manikin; S, source manikin) for the tests with the displacement diffuser (D) and the mixing diffuser (M), vertical measuring line (L1) and radiator (R). The position of the target manikin was moved to obtain the different separation distances. All measurements in meters

Table 5.1 Experimental tests with two manikins and displacement ventilation

Test	Position of the manikins	Distance between the manikins
1	Two manikins standing face to face	a) 0.35 m
		b) 0.50 m
		c) 0.80 m
		d) 1.10 m
2	Two manikins standing face to side	a) 0.35 m
		b) 0.50 m
		c) 0.80 m
		d) 1.10 m
3	Two manikins standing back to face	a) 0.35 m
		b) 0.50 m
		c) 0.80 m
		d) 1.10 m
4	Source sitting and target standing	a) 0.70 m
		b) 1.10 m

5.3.2 Results

The vertical temperature distribution in the room along the line L1 was measured for the displacement and mixing ventilation tests. The temperature conditions maintained for each of the tests are presented in figure 5.4, where it is possible to see a typical vertical temperature gradient for the displacement ventilation case.

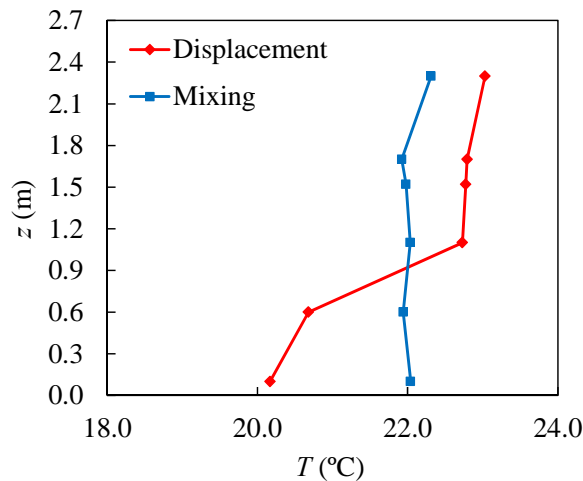


Figure 5.4 Vertical temperature distributions at L1 for the displacement and mixing ventilation tests

Figure 5.5 shows the concentration results for tests 1, 2, 3 and 4. For test 1, figure 5.5(a), which corresponds with the manikins facing each other, a clean area is maintained at the height of the chest in all the cases with an exposure level close to zero. This is typical of displacement ventilation, although the cleanest zone may be lower. Displacement ventilation can create a clean low zone, but it will also create a zone with higher concentration of exhaled contaminants because the exhalation is a weak heat source, see Li et al. (2011). This high level of concentration is shown in the exposure of the target manikin, reaching a maximum value of 12.0 at a separation distance of 0.35 m. However, this concentration exposure c_{exp}/c_R decreases as the separation distance increases.

This result is similar to the data obtained by Bjørn and Nielsen (2002) and Nielsen et al. (2008) for the face to face values, and it shows that the contaminated exhalation flow can penetrate the breathing zone of a standing person who faces the manikin, and produces an exposure level of several times the return concentration in the room. The concentration above the head of the target manikin is also high. This effect is provoked by the exhalation flow that rises due to the exhalation temperature and the temperature difference with the surrounding air.

Figure 5.5(b) shows the results for test 2, with the target manikin turned 90°. The exposure concentration c_{exp}/c_R is also high, with values very close to 7.0 and 6.0 for the separation distances of 0.35 m and 0.50 m respectively. However, the value is significantly reduced when the distance is more than 0.50 m. It is important to notice that the concentration values above the head of the target manikin are higher than the exposure values. The relative position of the target manikin may cause a different microenvironment and allow the contaminated exhalation flow to move upward above the head of the target manikin. The results close to zero at the chest height are due to the contaminant

stratification as discussed in test 1.

The target manikin has its back to the source in test 3. The results show that the exposure concentrations at all the separation distances are close to 1.0, which corresponds to a situation of fully mixed air, see figure 5.5(c). The exposure levels, and therefore the infection risk, are reduced significantly.

Personal exposure, c_{exp}/c_R , and concentration values above the target manikin, c_{10}/c_R , for test 4, which corresponds to the case with the source manikin seated, hardly vary with the distance, see figure 5.5(d). At the chest height the concentration value is directly influenced by the primary flow from the source manikin, which is exhaling the air at almost the same height as the chest, 1.23 m. When the source manikin is at 0.70 m from the target, the concentration of pollutants c_{chest}/c_R at the chest is almost 10. However, it is possible to see a significant decrease in the concentration value when the separation distance between the two manikins increases to 1.10 m. In this position, the exhaled air from the source manikin moves above chest height before reaching the chest of the target manikin.

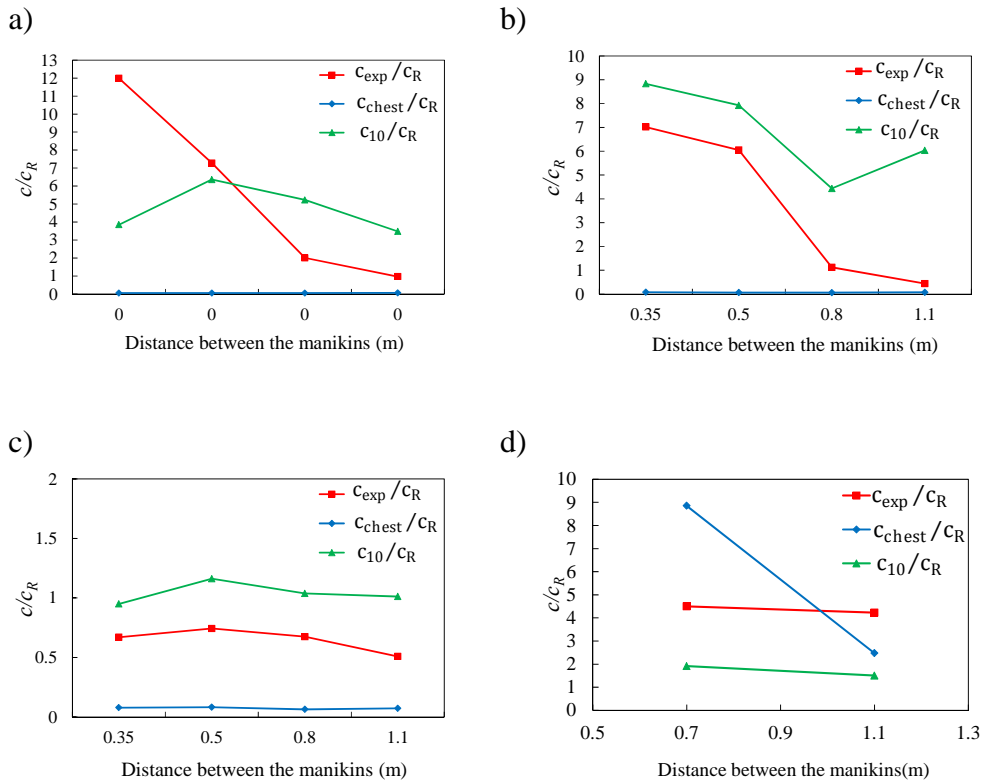


Figure 5.5 Comparison of the exposure concentration values in the inhalation (c_{exp}/c_R), the chest (c_{chest}/c_R), and above the target manikin (c_{10}/c_R) for the displacement ventilation tests a) test 1, b) test 2, c) test 3, d) test 4

5.3.3 Comparison of the personal exposure levels

Figure 5.6 shows the exposure of the target manikin, given as c_{exp}/c_R , where c_{exp} is the concentration in the target manikin's inhalation, and c_R is the return concentration.

For the face to back situation the value of c_{exp}/c_R is ~ 0.5 , which is due to the inhalation of the manikin from the low clean area of the room. The exposure is maintained at the same level for all the separation distances due to the lack of direct exposure from the source exhalation.

When the manikins are side to face and the separation distance is 1.10 m exposure value close to 0.5 is also obtained. However, when the distance decreases the concentration values increase significantly, reaching a maximum value close to 7.0 for the separation distance of 0.35 m.

The face to face test shows the largest exposure values. For distances lower than 0.80 m it is possible to see a remarkable increase in the direct exposure of the target manikin, due to the direct influence of the exhalation flow of the source manikin. This is a serious fact to take in consideration regarding the protection against cross-infection risk in rooms with this vertical temperature gradient.

Finally, when the source manikin is seated, the exposure value remains high, close to 5.0 for the two separation distances studied. This fact may be due to the low position of the source exhalation flow that rises to the upper part generating higher contaminant concentration level at the height of the target inhalation. A detailed description of the exhalation flow can be found in chapter 4.

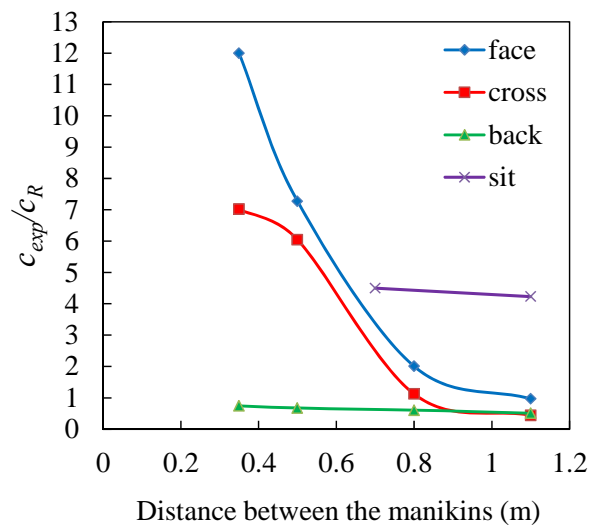


Figure 5.6 Comparison of the personal exposure obtained for the four displacement ventilation cases: face to face (face), face to side (cross), face to back (back) and with the source manikin seated (sit)

Figure 5.7 shows a comparison of the contaminant concentration data measured for the different relative positions over time and for the different separation distances.

It is possible to see that the peak values of concentration exposure are higher than the average values shown in the rest of figures. It means that the personal exposure at some

instants of time can be higher than the average values show in the rest of the graphs of this chapter.

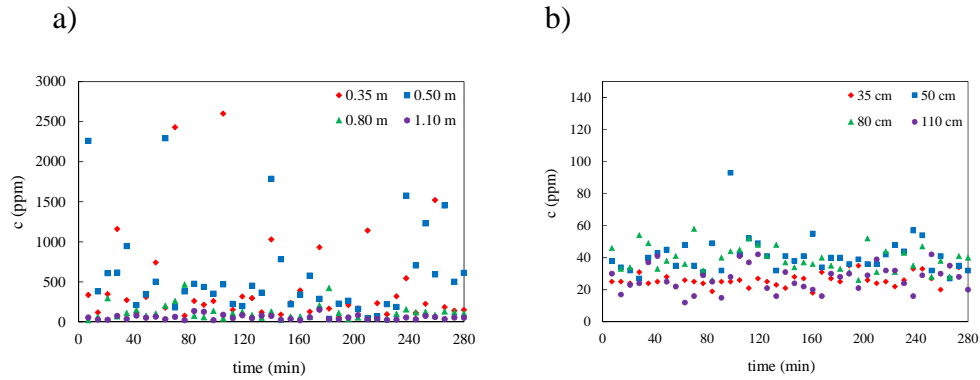


Figure 5.7 Concentration measurement over 280 minutes for two displacement ventilation tests a) test 1 (face to face), b) test 2 (face to back)

5.4 Two manikins within a room with mixing ventilation

5.4.1 Layout of the tests

For the study of the cross-infection risk between two people of the same height in a room with a mixing ventilation system, two relative positions between the manikins were studied: standing face to face and with the target manikin standing and the source manikin seated, see table 5.2. The placement of the manikins and the radiator was the same as for the displacement ventilation case see figure 5.3. The relative position of the source manikin respect to the radiator was maintained during the test while the target manikin was moved to obtain the four different separation distances: 0.35 m, 0.50 m, 0.80 m and 1.10 m.

Table 5.2 Experimental tests with two manikins and displacement ventilation

Test	Position of the manikins	Distance between the manikins
1	Two manikins standing face to face	a) 0.35 m
		b) 0.50 m
		c) 0.80 m
		d) 1.10 m
2	Source sitting and target standing	a) 0.70 m
		b) 1.10 m

The vertical temperature distribution measured in the room along the line L1 shows a typical temperature distribution of a mixing ventilation system, without any vertical gradient; see figure 5.4.

5.4.2 Results

The concentration results for tests 1 and 2 are shown in figure 5.8. For test 1, figure 5.8(a), the values of the exposure concentration, and the concentration at the chest of the target manikin, are observed to be around 1.0, which indicates a fully mixed value in the thermal plume around the target manikin and in the inhalation zone. However, although the concentration values above the head of the target manikin are around 1.0 for the largest distances, the pollution level increases when the separation distance is decreased to less than 0.80 m. This is due to a direct influence of the source manikin's exhalation flow in this area, especially when the separation distance is 0.35 m, where it is possible to observe a maximum value close to 1.4. These results agree with the observed location of the breathing flow profile in the mixing ventilation case, see chapter 4.

For test 2, see figure 5.8(b), the concentration results show values very close to 1.0 for all the separation distances, typical of a fully mixing case. A separation distance of 0.70 m between the manikins is enough to dilute the contaminants of the exhalation flow generating concentration values close to 1.0 at all the positions around the target manikin, the chest (c_{chest}/c_R), the inhalation (c_{exp}/c_R) and above the head (c_{10}/c_R).

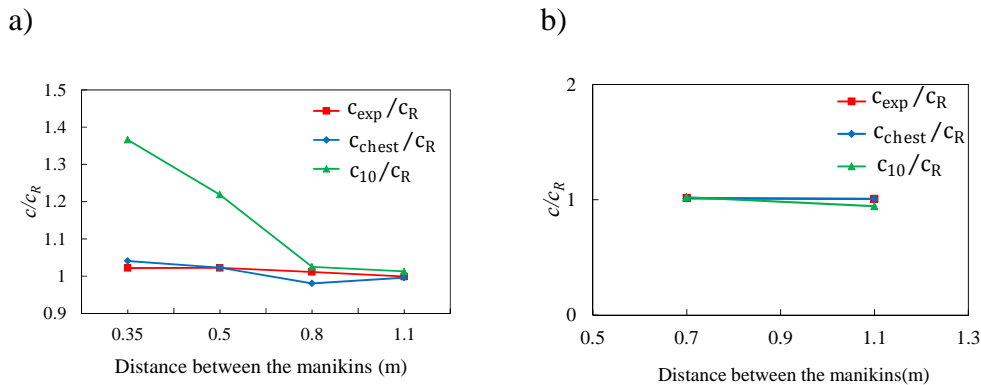


Figure 5.8 Comparison of the exposure concentration values in the inhalation (c_{exp}/c_R), the chest (c_{chest}/c_R), and above the target manikin (c_{10}/c_R) for the mixing ventilation tests a) test 1, b) test 2

5.5 Two manikins within a room without mechanical ventilation

Experimental tests with the manikins standing and facing each other in the room with no mechanical ventilation system were carried out. The placement of the manikins was the same than in the mixing and displacement ventilation cases, and the separation distances between them were: 0.35 m, 0.50 m, 0.80 m and 1.10 m.

The steady state conditions are, in this case, maintained by having an open door between

the laboratory and the test room. The temperature in the laboratory is maintained at $22\pm 1^\circ\text{C}$ by a radiator based heating system. The volume and size of the laboratory ensure the steady state conditions during the measuring period.

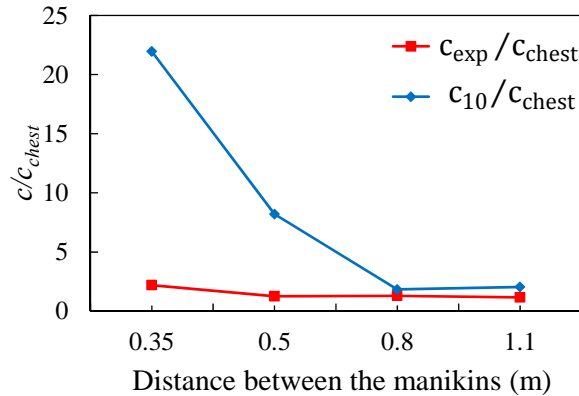


Figure 5.9 Comparison of the exposure concentration values in the inhalation (c_{exp}/c_{chest}) and above the target manikin (c_{10}/c_{chest})

As there is no ventilation with return flow, the concentrations in the inhalation area and above the head of the target manikin have been compared to the concentration of the air at the chest of the target manikin. The exposure concentration values c_{exp}/c_{chest} are kept around 1.0, except for the case with the smaller separation distance where the value obtained is 2.2, as is shown in figure 5.9. However, it is possible to see much higher values of gas concentration above the head of the manikin, especially at distances of 0.50 m and 0.35 m. The behaviour of the airflow in the room is controlled by convective flows and the boundary layers of the manikins. Because of that, a concentration of pollutants from the exhalation flow of the source manikin is built up above the head of the target manikin, and the exhalation flow will influence the measurements when the separation distance is reduced.

5.6 Two manikins within a room with low velocity vertical ventilation

5.6.1 Layout of the tests

This study consists of three experimental tests summarized in table 5.3, where different conditions in the room are changed. For tests 1 and 2, the manikins are placed in the downward flow area generated by the textile diffuser, while for the test 3 the manikins are placed in the upward flow area generated by the diffusers. The placement of the manikins for each test is shown in figure 5.10.

Table 5.3 Experimental tests with two manikins and low-impulse velocity ventilation

Test	Sketch of the manikins in the room	Distance between the manikins
1		a) 0.35 m b) 0.50 m c) 0.80 m d) 1.10 m
2		a) 0.35 m b) 0.50 m c) 1.10 m
3		a) 0.35 m b) 0.50 m c) 0.80 m d) 1.10 m

Figures in table 5.3 show the textile diffusers, the circular exhaust opening, the radiator, the source manikin (in red) and the target manikin exposed to the contaminants (in blue).

Four additional cases were carried out in the room and the results are addressed in paper VI. This section only describes the three more significant ones.

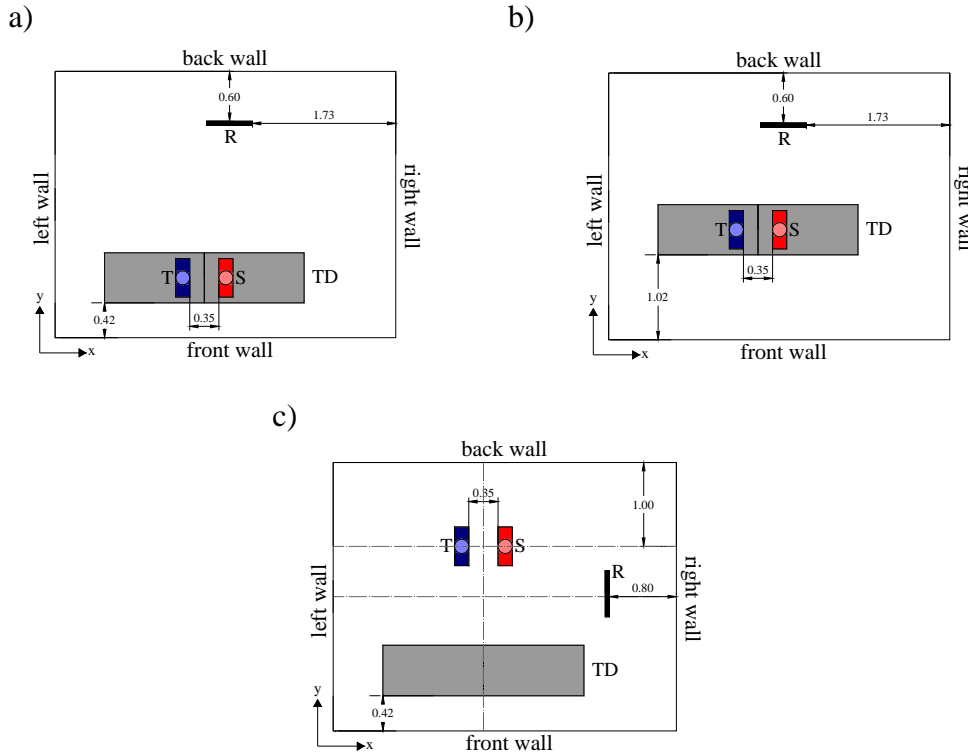


Figure 5.10 Layout of the room with the radiator (R), target manikin (T), source manikin (S) and textile diffuser (TD), a) test 1, b) test 2, c) test 3 (The distance between the manikins changed for the different tests)

5.6.2 Results

The results of the personal exposure, c_{exp}/c_R , and contaminant concentration at the chest, c_{chest}/c_R , and above the target manikin, c_{10}/c_R , for the different tests are shown in figure 5.11. Figure 5.11(a) shows a high exposure value, close to 6.0, for a distance of 0.35 m between the manikins. This may be due to the micro-environment generated by the manikins and observed with smoke visualization. More details about the micro-environment can be found in paper VI. The thermal plume of the two manikin at this short distance generate a significant upward flow that makes it difficult for the clean, supplied air to entrain the air between the manikins, reducing the mixing process. This phenomenon allows the contaminated exhalation flow from the source to penetrate the breathing area of the target manikin. The exposure decreases when the separation distance increases, as was found in the displacement ventilation tests. The concentration above the target manikin is maintained very low at all the distances due to the direct influence of the clean air from the diffuser. At the chest, the contaminant concentration is low and close to 1.0. For the separation distances of 0.35 m and 0.50 m the increase of the concentration values may be due to the

lack of influence of the air from the diffuser that also produces a high exposure.

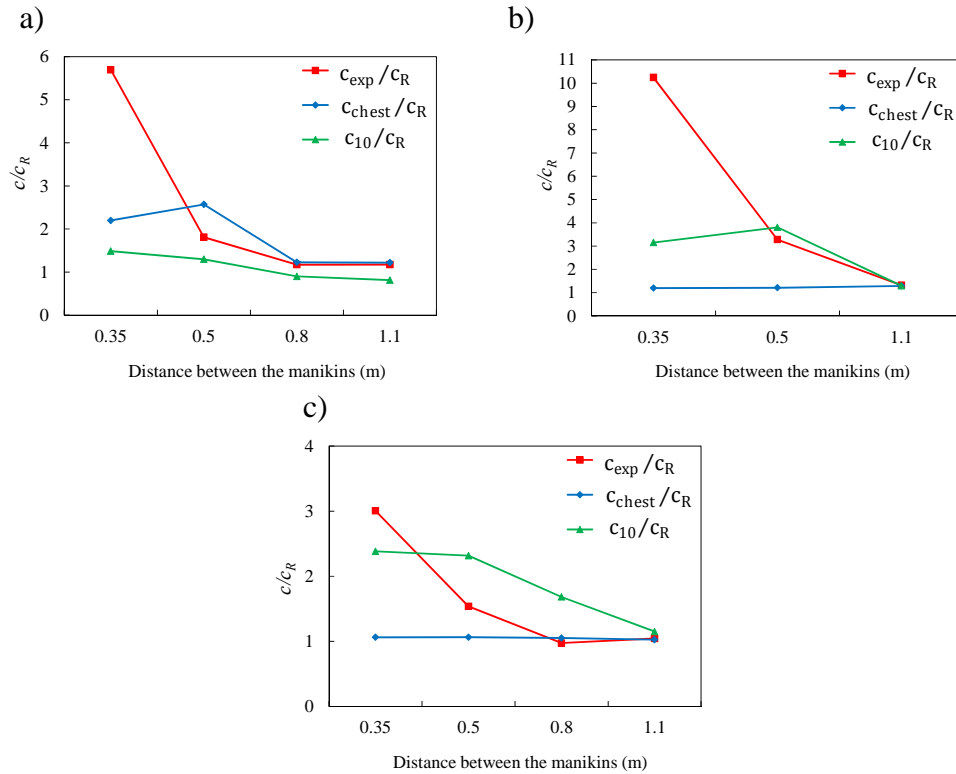


Figure 5.11 Comparison of the exposure concentration values in the inhalation (c_{exp}/C_R), the chest (c_{chest}/C_R), and above the target manikin (c_{10}/C_R) for the low-velocity vertical ventilation tests a) test 1, b) test 2, c) test 3

For test 2, the personal exposure values are significantly high, while the contaminant concentration at the height of the chest shows a value close to 1.0 for all the separation distances, see figure 5.11(b). This phenomenon may be due to the upward flow generated by the thermal plumes of the manikins, which deflect the clean, supplied air around the manikins and induce it to the upper part. In this way, the height of the chest is maintained clean and higher concentration values are found at the inhalation and above the manikin. The contaminant concentration in the inhalation of the target manikin is also directly influenced by the exhalation flow of the source manikin for a distance of 0.35 m.

It is important to notice the influence that the parallel wall close to the diffusers may have on the personal exposure. For test 1, the personal exposure values are lower than for test 2. This may be due to the influence of the wall that drives the downward flow generated by the diffuser close to the manikins and help to create a mixing process in the breathing area. A Coanda effect generated by this wall has been visualized with smoke and can be found in chapter 3.

Test 3 shows the results for the test where the two manikins are placed in the upward flow area of the room, see figure 5.11(c). The results show that c_{chest}/C_R is kept close to 1.0 at all the separation distances. The personal exposure, c_{exp}/C_R , is also kept close to 1.0 when the manikins are separated 0.80 m and 1.10 m. However, this value increases significantly

for 0.50 m and reaches a maximum value of 3.0 for 0.35 m. This maximum value is due, like in the rest of the cases, to the direct influence of the source exhalation flow that penetrates into the breathing area of the target manikin at this short distance, increasing the level of contaminants, even when the dominating airflow is upward. However, the personal exposure is lower than for the two downward cases studied, test 1 and 2. It is especially surprising that the protection from cross infection is larger in this area outside the vertical downward flow below the ceiling mounted diffuser. The measurements support the theory that upward or downward flow around the manikins has a strong influence on the exposure of the target manikin and it is a question on the deflection of the exhalation and an influence of the temperature difference. Experiments with manikins of different heights show a similar problem, namely the importance of the target manikin's location in the exhalation flow of the source manikin, Liu et al. (2010).

The contaminant concentration above the target manikin, c_{10}/c_R , are the maximum value obtained in tests with a separation distance of 0.50 m, 0.80 m and 1.10 m. For a distance of 0.35 m reaches a maximum value, close to 2.5. The high values produced at this location are due to the upward flow generated by the room air flow and the exhalation flow. Contaminants rise to the upper part of the room, keeping the chest and breathing area free of contaminants.

5.7 Comparison of the results for the different ventilation strategies

The relation between the personal exposure to exhaled contaminants and different ventilation strategies (local temperature distributions) in a room has been analyzed. Figure 5.12 compares the exposure of the target manikin with the different ventilation systems.

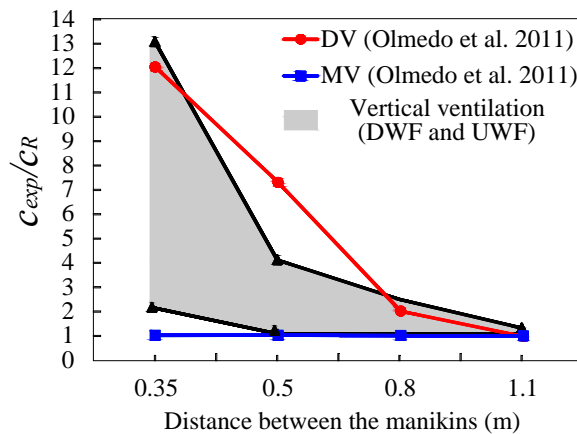


Figure 5.12 Comparison of the personal exposure concentration values for the different ventilation systems studied: displacement ventilation (DV), mixing ventilation (MV) and low-velocity vertical ventilation (grey area)

The distance between the two thermal manikins used to simulate two standing people in a room has been varied. The separation distance has been found to be a key factor in the risk of cross-infection between two people (both exhaling through the mouth). For all the

ventilation strategies used, a separation distance higher than 0.8 m decreases significantly the personal exposure of the target manikin.

The displacement ventilation system produces a large contaminant concentration at the height of the breathing provoked by the “lock-up phenomenon”. The vertical thermal stratification generated by this kind of systems maintains the exhaled contaminants trapped at the height of the breathing zone. This fact produces a high risk of airborne cross-infection to the target manikin, which is significantly high at distances lower than 0.8 m. However the mixing ventilation maintains a more stable contaminant concentration in the breathing area of the target manikin for all the separation distances. The mixing process and the temperature difference produce a dilution and a direction of the exhaled contaminants in the air that maintains the personal exposure at lower levels irrespective of the distance between the manikins.

Finally, the downward flow ventilation is supposed to create a protection against the airborne cross-infection to the target manikin. However, the results show that the thermal plumes created by the thermal manikins disturb the downward flow and can induce a mixing process in the room. The personal exposure varies in a wide range for the different cases studied, which show that the layout of the room and the relative position of people is a factor to take into account if the risk of airborne cross-infection wants to be reduced.

CHAPTER 6

Conclusions and future work

Following are the conclusions and proposals for future work that are deduced from the research made within this thesis.

The human exhalation flow and the dispersion of exhaled contaminants in a room have been analyzed using different ventilation strategies: displacement ventilation, mixing ventilation, non-mechanical ventilation and low-velocity vertical ventilation.

The different air distribution systems create a different micro-environment around the thermal manikin and especially around its breathing area. This fact makes the exhalation flows with different trajectories for the different ventilation systems. The vertical temperature gradient connected to a displacement ventilation system retains the exhalation at head height of surrounding persons, while mixing ventilation allows the exhalation to rise above head height due to temperature difference between exhalation and the surrounding air. This temperature difference is directly connected to the direction of the exhalation flow.

The exhalation flow can be described by simple expressions, using the peak velocity and peak mean concentration values, which show these variables as proportional to the reciprocal horizontal distance from the mouth.

Experiments with cross infection risk between two persons (source manikin and target manikin) show that the air distribution systems and especially the microenvironment they create are of importance to the exhalation flow between the manikins.

The relative positions as well as the separation distance between the manikins have been found to be key factors in order to reduce the risk of airborne cross-infection between people in a room. For a downward ventilation system it is also important the relative position of the people respect to the diffuser as well as the layout of the room.

Neither the displacement ventilation nor the downward ventilation systems produce any special protection to cross-infection when the separation distance between people (manikins) is lower than 0.80 m.

The possibility of realizing numerical simulations to study the airborne route of cross-infection between people in a room would be a very powerful tool. This offers many possibilities for the study of airflow patterns and dispersion of exhaled contaminants. Many parameters that may influence the risk of airborne cross-infection in a room should be taken into account in future works with numerical or experimental results, such as: breathing functions, difference in heights of people, number of people in a room, activity level of persons or air velocity and turbulence level in the micro-environment around the persons.

Bibliography

- Badeau, A., Afshari, A., Goldsmith, T. and Frazer, D. (2002) Preliminary prediction of flow and particle concentration produced from natural human cough dispersion, *Proceedings of the Second Joint EMBS/BMES Conference*, Houston, USA , 23-26.
- Baturin, V.V. (1972) *Fundamentals of Industrial Ventilation*, Oxford, New York, Pergamon Press.
- Bjørn, E. (1999) Simulation of human respiration with breathing thermal manikin, *Proceedings of Third International Meeting on Thermal Manikin Testing*, Stockholm, Sweden, National Institute for Working Life, 78-81.
- Bjørn, E. and Nielsen, P.V. (2002) Dispersal of exhaled air and personal exposure in displacement ventilated room, *Indoor Air*, **12**, 147-164.
- Brohus, H. and Nielsen, P.V. (1996) Personal exposure in displacement ventilated rooms, *Indoor Air*, **6**, 157-167.
- CDC (2003) *Guidelines for Environmental Infection Control in Health-Care facilities*, USA, U.S. Department of health and human services centers for disease control and prevention (CDC).
- CDC (2005) *Guidelines for preventing the transmission of Mycobacterium tuberculosis in Health-Care Settings*, USA, U.S. Department of health and human services centers for disease control and prevention (CDC).
- Chao, C. Y. H., Wan, M. P. and Sze To, G. N. (2008) Transport and removal of expiratory droplets in hospital ward environment, *Aerosol. Sci. Technol.*, **42**(5), 377-394.
- Chao, C. Y. H., Wan, M. P., Morawska, L., Johnson, G. R., Ristovski, Z. D., Hargreaves, M., Mengersen, K., Corbett, S., Li, Y., Xie, X. and Katoshevski, D. (2009) Characterization of expiration air jets and droplet size distributions immediately at the mouth opening, *J. Aerosol Sci.*, **40**, 122-133.

- Chen, Q., and Moser, A. (1991) Simulation of a multiple-nozzle diffuser, *Proc. of 12th AIVC Conference*, **2**, 1-14.
- Chen, C., Zhao, B., Cui, W., Dong, L., An, N. and Ouyang, X. (2010) The effectiveness of an air cleaner in controlling droplet/aerosol particle dispersion emitted from a patient's mouth in the indoor environment of dental clinics, *J.R. Soc. Interface*, **7**, 1105-1118.
- Chen, C. and Zhao, B. (2010) Some questions on dispersion of human exhaled droplets in ventilation room: answers from numerical investigation, *Indoor Air*, **20**, 95-111.
- Cheong, K.W.D. and Phua, S.Y. (2006) Development of ventilation design strategy for effective removal of pollutant in the isolation room of a hospital, *Build. Environ.*, **41**, 1161-1170.
- Chow, T.T. and Yang, X.Y. (2004) Ventilation performance in operating theatres against airborne infection: review of research activities and practical guidance, *J. Hosp. Infect.*, **56**, 85-92.
- Chung, K.C. and Hsu, S.P. (2001) Effect of ventilation pattern on room air and contaminant distribution, *Build. Environ.*, **36**(9), 989-998.
- Clark, R.P. and Edholm, O.G. (1985) *Man and his thermal environment*, London, E. Arnold Publishing Co.
- Craven, B.A. and Settles, G.S. (2006) A computational and experimental investigation of the human thermal plume, *J. Fluids Eng.*, **128**(6), 1251-1259.
- Effros, R. M., Wahlen, K. and Bosbous, M. (2002) Dilution of respiratory solutes on exhaled condensates, *Am. J. Resp. Crit. Care*, **165**, 663-669.
- Einberg, G. and Hagstrom, K. (2005) CFD modelling of an industrial air diffuser - predicting velocity and temperature in the near zone. *Build. Environ.*, **40**(5), 601-615.
- Gao, N. and Niu, J. (2006) Transient CFD simulation of the respiration process and inter-person exposure assessment, *Build. Environ.*, **41**, 1214-1222.
- Gao, N. and Niu, J. (2007) Modeling particle dispersion and deposition in indoor environments, *Build. Environ.*, **41**, 3862-3876.
- Gupta, J.K., Lin, C. and Chen, Q. (2009) Flow dynamics and characterization of a cough, *Indoor Air*, **19**, 517-525.
- Gupta, J.K., Lin, C. and Chen, Q. (2010) Characterizing exhaled airflow from breathing and talking, *Indoor Air*, **20**, 31-39.

Hayashi, T., Ishizu, Y., Kato, S. and Murakami, S. (2002) CFD analysis on characteristics of contaminated indoor air ventilation and its application in the evaluation of the effects of contaminant inhalation by a human occupant, *Build. Environ.*, **37**, 219-230.

He, G., Yang, X. and Srebric, J. (2005) Removal of contaminants released from room surfaces by displacement and mixing ventilation: modeling and validation, *Indoor Air*, **15**, 367-380.

Huo, Y. and Haghghat, F. (2000) A systematic approach to describe the air terminal device CFD simulation for room air distribution analysis, *Build. Environ.*, **35**(6), 563-576.

ISO:7730 (2005) *Ergonomics of the thermal environment—Analytical determination and interpretation of thermal comfort using calculation of the PMV and PPD indices and local thermal comfort criteria*, 1-52, Switzerland.

Jensen, R.L., Pedersen, D.N., Nielsen, P.V. and Topp, C. (2001) Personal exposure between people in a mixing ventilated room, *Proceedings of the 4th International Conference on Indoor Air Quality, Ventilation & Energy Conservation I*: 33–40. Hunan University.

Jiang, Z., Chen, Q. and Moser, A. (1992) Comparison of Displacement and Mixing Diffusers, *Indoor Air*, **2**, 168–179.

Koskela, H. (2004) Momentum source model for CFD - simulation of nozzle duct air diffuser, *Energ. Buildings*, **36**, 1011-1020.

Lee, E., Khan, J.A., Feigley, C.E., Ahmed, M.R. and Hussey, J.R. (2007) An investigation of air inlet types in mixing ventilation, *Build. Environ.*, **42**, 1089-1098.

Li, Y., Yu, I.T.S., Xu, P., Lee, J.H.W., Wong, T.W., Ooi P.L. and Sleigh A.C. (2004) Predicting super spreading events during the 2003 Sever Acute Respiratory Syndrome epidemics in Hong Kong and Singapore, *Am. J. Epidemiol.*, **160**(8), 719-728.

Li, Y., Huang, X., Yu, I.T.S., Wong, T.W. and Qian, H. (2004) Role of air distribution in SARS transmission during largest nosocomial outbreak in Hong Kong, *Indoor Air*, **15**, 83-95.

Li, Y., Leung, G.M., Tang, J.W., Yang, X., Chao, C.Y.H., Lin, J.Z., Lu, J.W., Nielsen, P.V., Niu, J., Qian, H., Sleigh, A.C., Su, H.-J.J., Sundell, J., Wong, T.W. and Yuen, P.L. (2007) Role of ventilation in airborne transmission of infectious agents in the built environment - a multidisciplinary systematic review, *Indoor Air*, **17**, 2-18.

Li, Y., Nielsen, P.V. and Sandberg, M. (2011) Displacement ventilation in hospital environments, *Ashrae J.*, **53**(6), 86-88.

Lim, T., Cho, J. and Kim, B.S. (2010) The predictions of infection risk of indoor airborne transmission of diseases in high-rise hospitals: tracer gas simulation, *Energ. Buildings*, **42**, 1172–1181.

Liu, L., Li, Y., Nielsen, P.V., Jensen, R.L., Litewnicki and M. and Zajas, J. (2009) An experimental study of human exhalation during breathing and coughing in a mixing ventilated room, *Proc. 9th Int. Conf. Healthy Buildings*, Syracuse, NY, USA.

Liu, J., Wang, H. and Wen, W. (2009) Numerical simulation on a horizontal airflow for airborne particles control in hospital operating room, *Build. Environ.*, **44**, 2284-2289.

Liu, L., Li, Y., Nielsen, P.V. and Jensen, R.L. (2010) An experimental study of exhaled substance exposure between two standing manikins, *Proceedings of 16th ASHRAE IAQ Conference*, Kuala Lumpur, Malaysia.

Morawska, L. (2006) Droplet fate in indoor environments, or can we prevent the spread of infection?, *Indoor Air*, **16**, 335-347.

Morawska, L., Johnson, G.R., Ristovski, Z.D., Hargreaves, M., Mengersen, K., Corbett, S., Chao, C.Y.H., Li, Y. and Katoshevski, D. (2009) Size distribution and sites of origin of droplets expelled from the human respiratory tract during expiratory activities, *J. Aerosol Sci.*, **40**, 256-269.

Mui, K.W., Wonga, L.T., Wu, C.L. and Lai, A.C.K. (2009) Numerical modeling of exhaled droplet nuclei dispersion and mixing in indoor environments, *J. Hazardous Materials*, **167**, 736-744.

Murakami, S. (2004) Analysis and design of micro-climate around the human body with respiration by CFD, *Indoor Air*, **14**(7), 144–156.

Nicas, M., Nazaroff, W.W. and Hubbard, A. (2005) Toward understanding the risk of secondary airborne infection: Emission of respirable pathogens, *J. Occup. Environ. Hyg.*, **2**, 143-154.

Nielsen, P.V. (1995) Lecture notes on mixing ventilation, Department of Building Technology and Structural Engineering, Aalborg University, Aalborg, Denmark.

Nielsen P.V. (1997a) The box method – a practical procedure for introduction of an air terminal device in CFD calculation. Department of Building Technology and Structural Engineering, Aalborg University, Aalborg, Denmark.

Nielsen, P.V. (1997b) The prescribed velocity method - A practical procedure for introduction of an air terminal device in CFD calculation. Department of Building Technology and Structural Engineering, Aalborg University, Aalborg, Denmark.

Nielsen, P.V. (2000) Velocity distribution in a room ventilated by displacement ventilation and wall-mounted air terminal devices, *Energ. Buildings*, **31**, 179–187.

Nielsen, P.V. (2007) Analysis and design of room air distribution systems. *HVAC&R. Res.*, **13**(6), 987-997.

Nielsen, P.V., Bartholomaeussen, N.M., Jakubowska, E., Jiang, H., Jonsson, O.T., Krawiecka, K., Mierzejewski, A., Thomas, S.J., Trampczynska, K., Polak, M. and Soennichsen, M. (2007) Chair with integrated personalized ventilation for minimizing cross infection, *Proceedings of 10th International Conference on Air Distribution in Rooms*, Helsinki, Finland.

Nielsen, P.V., Buus, M., Winther, F.V. and Thilageswaran, M. (2008) Contaminant flow in the microenvironment between people under different ventilation conditions, *ASHRAE Trans.*, **114**, part 2.

Nielsen, P.V. (2009) Control of airborne infectious diseases in ventilated spaces, *J.R. Soc. Interface*, **6**, 747-755.

Nielsen, P.V., Jensen, R.L., Litewnicki and M. and Zajas, J. (2009) Experiments on the microenvironment and breathing of a person in isothermal and stratified surroundings, *Proc. 9th Int. Conf. Healthy Buildings*, Syracuse, NY, USA.

Nielsen, P.V., Li, Y., Buus, M. and Winther, F.V. (2010) Risk of cross-infection in a hospital ward with downward ventilation, *Build. Environ.*, **45**, 2008–2014.

Nielsen, P.V., Olmedo, I., Ruiz de Adana, M., Grzelecki, P. and Jensen R.L. (2011) Airborne cross infection between two people in a displacement ventilated room, *Int. J. HVAC & R Res.* (in press).

Olmedo, I., Nielsen, P.V., Ruiz de Adana, M., Jensen, R.L. and Grzelecki, P. (2011) Distribution of exhaled contaminants and personal exposure in a room using three different air distribution strategies, *Indoor Air*, doi: 10.1111/j.1600-0668.2011.00736.x.

Qian, H., Li, Y., Nielsen, P.V., Hyldgaard, C.E., Wong, T.W. and Chwang, A.T.Y. (2006) Dispersion of exhaled droplet nuclei in a two-bed hospital ward with three different ventilation systems, *Indoor Air*, **16**, 111-128.

Qian, H., Li, Y., Nielsen, P.V. and Hyldgaard, C.E. (2008) Dispersion of exhalation pollutants in a two-bed hospital ward with a downward ventilation system. *Build. Environ.*, **43**, 344–354.

Qian, H. and Li, Y. (2010) Removal of exhaled particles by ventilation and deposition in a multibed airborne infection isolation room. *Indoor Air*, **20**, 284-297.

- Richmond-Bryant, J. (2009) Transport of exhaled particulate matter in airborne infection isolation rooms, *Build. Environ.*, **44**, 44–55.
- Roy, C.J and Milton, D.K. (2004) Airborne Transmission of communicable infection — The elusive pathway, *New Engl. J. Med.*, **350**(17), 1710-1712.
- Schwarz, K., Biller, H., Windt, H., Koch, W. and Hohlfeld J.M. (2010) Characterization of exhaled particles from the healthy human lung — A systematic analysis in relation to pulmonary function variables, *J. Aerosol Med.*, **23**(6), 371-379.
- Srebric, J. and Chen, Q. (2002) Simplified numerical models for complex air supply diffusers, *HVAC&R. Res.*, **8**(3), 277-294.
- Srebric, J., Vukovica, V., He, G. and Yang, X. (2008) CFD boundary conditions for contaminant dispersion, heat transfer and airflow simulations around human occupants in indoor environments, *Build. Environ.*, **43**, 294-303.
- Tang, J., Liebner, T., Brent, C. and Gary, S. (2009) A schlieren optical study of the human cough with and without wearing a mask for aerosol infection control, *J.R. Soc. Interface*, **6**, 727-736.
- Tang, J.W., Noakes, C.J., Nielsen, P.V., Eames, I., Nicolle, A., Li, Y. and Settles, G.S. (2011) Observing and quantifying airflows in the infection control of aerosol - and airborne-transmitted diseases: an overview of approaches, *J. Hosp. Infect.*, **77**, 213-222.
- Wan, M. P. and Chao, C. Y. H. (2007) Transport characteristics of expiratory droplet nuclei in indoor environments with different ventilation airflow patterns, *J. Biomech. Eng.*, **129**, 341-353.
- Wan, M.P., Sze To, G. N., Chao, C. Y. H., Fang, L., and Melikov, A. (2009) Modeling the fate of expiratory aerosols and the associated infection risk in an aircraft cabin environment. *Aerosol Sci. Tech.*, **43**, 322-343.
- Wells, W.F. (1934) On air-borne infection. Study II. Droplets and droplet nuclei, *Am. J. Hyg.*, **20**, 611–618.
- Woloszyn, M, Virgone, J. and Mélen, S. (2004) Diagonal air-distribution system for operating rooms: experiment and modeling, *Build. Environ.*, **39**, 1171-1178.
- Xie, X., Li, Y., Chwang, A.T.Y., Ho, P.L. and Seto, W.H. (2007) How far droplets can move in indoor environments – revisiting the Wells evaporation-falling curve, *Indoor Air*, **17**, 221–225.

Yang, Y., Sze-To, G.N. and Chao, C.Y.H. (2011) Estimation of the aerodynamic sizes of single bacterium-laden expiratory aerosols using stochastic modeling with experimental validation, *Aerosol. Sci. Technol.*, **46**(1), 1-12.

Yin, Y., Gupta, J.K., Zhang, X., Liu, J. and Chen Q. (2011) Distributions of respiratory contaminants from a patient with different postures and exhaling modes in a single - bed inpatient room, *Build. Environ.*, **46**(1), 75-81.

Yu, I.T.S., Li, Y., Wong, T.W., Tam, W., Phil, M., Chan, A.T., Lee, J.H.W., Leung D.Y.C. and Ho, T. (2004) Evidence of airborne transmission of the Severe Acute Respiratory Syndrome virus, *New Engl. J. Med.*, **350**(17), 1731-1739.

Zhao, B., Zhang, Z. and Li, X (2005) Numerical study of the transport of droplets or particles generated by respiratory system indoors, *Build. Environ.*, **40**, 1032-1039

Zhu, S., Kato, S., Murakami, S. and Hayashi, T. (2005) Study on inhalation region by means of CFD analysis and experiment, *Build. Environ.*, **40**, 1329–1336.

Zhu, K., Kato, S. and Yang, J. (2006a) Investigation into airborne transport characteristics of airflow due to coughing in a stagnant indoor environment, *ASHRAE Trans.*, **112**(2), 123-133.

Zhu, K., Kato, S. and Yang, J. (2006b) Study on transport characteristics of saliva droplets produced by coughing in a calm indoor environment, *Build. Environ.*, **41**, 1691–1702.

Zhu, K. and Kato, S. (2006) Investigating how viruses are transmitted by coughing, *ASHRAE IAQ Applications*, **7**, 3-6.

Zukowska, D., Melikov, A. and Popiolek, Z. (2008) Impact of thermal plumes generated by occupant simulators with different complexity of body geometry on airflow pattern in rooms, *Proc. 7th Int. Thermal Manikin and Modeling Meeting*, Coimbra, Portugal.

Appendix A

Calibration of the equipment

A. 1 Calibration of the thermocouples

During the experiments several thermocouples were used to measure the temperature at different positions in the room. Before that, the thermocouples were calibrated in order to obtain an accurate value of temperature.

Two calibrate the thermocouples two devices were used:

- ✓ Precision thermometer used to measure the temperature of reference for the thermocouples, see figure A.1 (a).
- ✓ Thermal calibration bath, ISOCAL 6, manufactured by Isotech. This device allowed the calibration of three thermocouples at the same time, see figure A.1 (b).



Figure A.1 a) Precision thermometer used for the calibration of the thermocouples, b) Thermal calibration bath, ISOCAL 6

After a stabilization time of about 15 minutes, the temperature calibration device maintained the bath temperature stable in order to compare the measurements of three thermocouples with the measurement of the precision thermometer. This process was carried out at three different temperatures: 15°C, 30°C and 45°C to obtain the calibration curve and the corresponding calibration equation for each thermocouple. The calibration curve/equation compares the measurements values of the precision thermometers with each thermocouple. The measurements of the thermocouples are adjusted to a linear equation of the following type:

$$T_r = a + bT_m \quad (\text{A.1})$$

where T_r is the temperature measured by the precision thermometer and T_m is the temperature measured by the thermocouples.

Figure B.2 shows one of the calibration curve and equation obtained for one of the thermocouple type K.

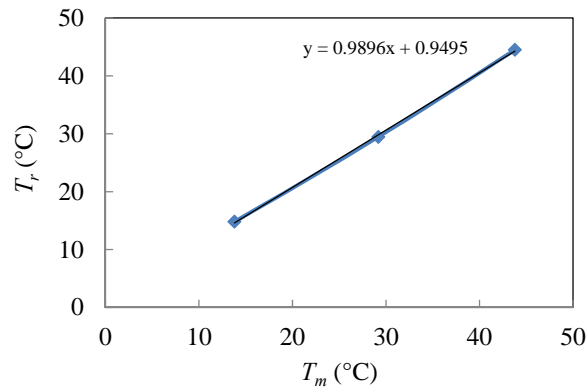


Figure A.2 Calibration curve and equation obtained for one of the thermocouples

The calibration curve of each thermocouple was used in the post-process of the temperature data of all the experiments.

A.2 Calibration of the anemometers

Hot sphere anemometers, DANTEC 54R50 were used to measure the velocity of the air at different positions in the room during the experiments. Results of measurements were logged in a computer with the corresponding DANTEC software, see figure A.3.

Additionally, for the calibration process of the anemometers a wind tunnel was used to expose the anemometers to a fixed velocity using different orifice plates, see figure A.4.

During this process the computer software measured the voltage difference generated by the anemometers while a manometer connected to the wind tunnel measured the pressure difference (true velocity).

The measured pressure difference was related by a linear equation with the velocity of the air (true velocity).

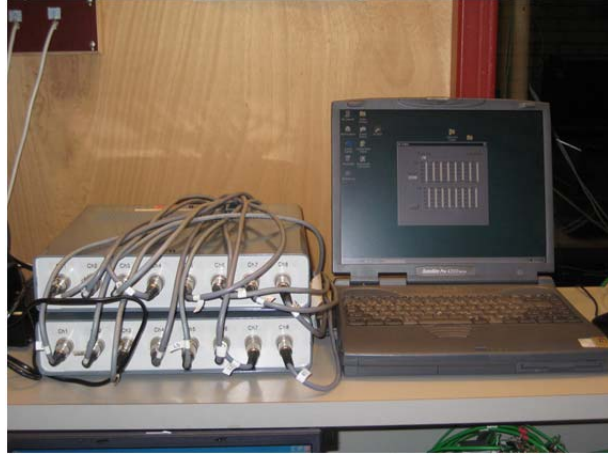


Figure A.3 Anemometers connected to the computer

A calibration curve established a relation between the voltage and the true velocity measured by the thermocouples and the manometer, respectively, that is added in the computer software to take the velocity measurements.



Figure A.4 Wind tunnel where the anemometers were placed to be calibrated

Appendix B

Study of the human breathing flow profile in a room with three different ventilation strategies

The paper presented in this Appendix is published in the *16th ASHRAE IAQ Conference "Airborne Infection Control – Ventilation, IAQ & Energy"*, Kuala Lumpur/ Malaysia 10-12 November 2010.



Appendix C

Airborne cross-infection risk between two people standing in surroundings with a vertical temperature gradient

Paper published in *HVAC & Research*, **18**(4):1-10.

Peter V. Nielsen, Inés Olmedo, Manuel Ruiz de Adana, Piotr Grzelecki, and Rasmus L. Jensen (2012)

ABSTRACT: The transmission of exhaled small particles from one person to another in an indoor environment can take place both directly (in the microenvironment around the persons) and via the room air distribution. The impact of these transmission routes for two persons is investigated in detail by evaluating the exposure to gaseous substances (simulating particles $<5 \mu\text{m}$) in a room with a vertical temperature gradient obtained by displacement ventilation. Experiments are conducted with two breathing thermal manikins—one the source and the other the target. In the experiments, the distance between the two manikins varies from 1.1 to 0.35 m (43 to 14 in.). A tracer gas N₂O is used to represent the gaseous substances exhaled by the source manikin. The concentration of N₂O is measured to study the impact on the exposure of the distance between manikins and manikin positions (face to face, face to the side of the target manikin, face to the back of the target manikin, and a seated source manikin). The exposure increases with decreasing distance between the manikins, and the highest values are obtained in the face-to-face position. Face to the side also creates some exposure of the target manikin, while face toward the target manikin's back does not give any direct exposure through the microenvironment. The thermal stratification in the room supports a significant exposure of the target manikin when the source manikin is seated and breathing toward the chest of a standing manikin.

DOI: 10.1080/10789669.2011.598441

Appendix D

Airflow pattern generated by three air diffusers: Experimental and visual analysis

The paper presented in this Appendix is published in the *6th Mediterranean Congress of Climatization*, Madrid/Spain 2-3 June 2011.



**VI MEDITERRANEAN CONGRESS
OF CLIMATIZATION**

Madrid, 2 - 3 June 2011

Appendix E

Experimental study about how the thermal plume affects the air quality a person breathes

The paper presented in this Appendix is published in the *12th International Conference on Air Distribution*, Trondheim/Norway 19-22 June 2011.



ROOMVENT 2011



Appendix F

Distribution of exhaled contaminants and personal exposure in a room using three different air distribution strategies

Paper published in *Indoor Air*, **22**(1), 64-76

Inés Olmedo, Peter V. Nielsen, Manuel Ruiz de Adana, Piotr Grzelecki, and Rasmus L. Jensen (2012)

ABSTRACT: The level of exposure to human exhaled contaminants in a room depends not only on the air distribution system but also on people's different positions, the distance between them, people's activity level and height, direction of exhalation, and the surrounding temperature and temperature gradient. Human exhalation is studied in detail for different distribution systems: displacement and mixing ventilation as well as a system without mechanical ventilation. Two thermal manikins breathing through the mouth are used to simulate the exposure to human exhaled contaminants. The position and distance between the manikins are changed in order to study the influence on the level of exposure. The results show that the air exhaled by a manikin flows a longer distance with a higher concentration in case of displacement ventilation than in the other two cases, indicating a significant exposure to the contaminants for one person positioned in front of another. However, in all three cases the exhalation flow of the source penetrates the thermal plume, causing an increase in the concentration of contaminants in front of the target person. The results are significantly dependent on the distance and position between the two manikins in all three cases.

DOI: 10.1111/j.1600-0668.2011.00736.x.

Appendix G

The risk of airborne cross infection in a room with vertical low-velocity ventilation

Paper published in *Indoor Air*

Inés Olmedo, Peter V. Nielsen, Manuel Ruiz de Adana and Rasmus L. Jensen (2012)

ABSTRACT: Downward flow ventilation systems are one of the most recommended ventilation strategies when contaminants in rooms must be removed and people must be protected from the risk of airborne cross-infection. This study is based on experimental tests carried out in a room with downward flow ventilation. Two breathing thermal manikins are placed in a room face to face. One manikin's breathing is considered to be the contaminated source in order to simulate a risky situation with airborne cross infection. The position of the manikins in relation to the diffuser, the location of diffuser in the room as well as the distance between the manikins are being changed to observe the influence of these factors on the personal exposure of the target manikin. The results show that the downward flow in different situations often is unable to penetrate the microenvironment generated by the manikins. The downward ventilation system can give an unexpected high level of contaminant exposure of the target manikin, when the distance between the manikins is reduced.

DOI: 10.1111/j.1600-0668.2012.00794.x.

Appendix H

Analysis of the IEA 2D test. 2D, 3D steady or unsteady airflow?

Technical report. Series number 106, Department of Civil Engineering, Aalborg University, September 2010.